



Hot-dip-zinc-coating of prefabricated structural steel components

M. Feldmann, T. Pinger, D. Schäfer, R. Pope, W. Smith, G. Sedlacek

Background document in support to the implementation, harmonization and further development of the Eurocodes



Joint Report

Prepared under the JRC – ECCS cooperation agreement for the evolution of Eurocode 3
(programme of CEN / TC 250)

Editors: G. Sedlacek, M. Gérardin, A. Pinto, H. Varum

EUR 24286 EN - 2010

The mission of the JRC-IPSC is to provide research results and to support EU policy-makers in their effort towards global security and towards protection of European citizens from accidents, deliberate attacks, fraud and illegal actions against EU policies.

European Commission
Joint Research Centre
Institute for the Protection and Security of the Citizen

Contact information

Address: Joint Research Centre, ELSA Unit, TP 480, 21027 Ispra (Va), Italy
E-mail: michel.geradin@jrc.ec.europa.eu
Tel.: +39 (0332) 78 9989
Fax: +39 (0332) 78 9049
<http://ipsc.jrc.ec.europa.eu/>
<http://www.jrc.ec.europa.eu/>

The European Convention For Constructional Steelwork (ECCS) is the federation of the National Associations of Steelwork Industries. The aim of ECCS is to promote the use of steelwork in the construction sector by the development of technical and promotional information. The ECCS covers a worldwide network of partners in the Steel Industry: Producers, Fabricators, Contractors and Experts, Universities and Research Institutes.
<http://www.steelconstruct.com/>

Contact information

Address: Mies-van-der-Rohe-Straße 1, D-52074 Aachen
E-mail: sed@stb.rwth-aachen.de
Tel.: +49 241 80 25177
Fax: +49 241 80 22140
<http://www.stb.rwth-aachen.de>

Legal Notice

Neither the European Commission nor any person acting on behalf of the Commission is responsible for the use which might be made of this publication.

***Europe Direct is a service to help you find answers
to your questions about the European Union***

**Freephone number (*):
00 800 6 7 8 9 10 11**

(* Certain mobile telephone operators do not allow access to 00 800 numbers or these calls may be billed.

A great deal of additional information on the European Union is available on the Internet. It can be accessed through the Europa server <http://europa.eu/>

JRC 56810

EUR 24286 EN
ISBN 978-92-79-15237-5
ISSN 1018-5593
DOI 10.2788/73644

Luxembourg: Office for Official Publications of the European Communities

© European Union, 2010
© European Convention for Constructional Steelworks, 2010

Reproduction is authorised provided the source is acknowledged

Printed in Italy

Acknowledgements

This report gives a survey on the state of the art concerning „Liquid metal assisted cracking“ of prefabricated structural steel components in the hot zinc bath and conclusions for a quantitative assessment procedure to avoid such cracking. It has been prepared on the basis of various sources:

- RFCS-CR-03021 Research project: “Failure mechanisms during Galvanizing”,
- Reports from research projects funded by Arbeitsgemeinschaft industrieller Forschung (AiF) No. 14545 N/1 and 265 ZBG/1,
- Research reports from various origins mentioned in the bibliography,
- Industry Guidance’s in UK, Austria, Japan, Canada and Germany,
- DAST-Richtlinie 022: Hot-dip zinc coating of prefabricated steel components,
- Numerous discussions held with representatives of Regulatory Bodies, industry and research institutes,
- Several doctoral thesis’ mentioned in the bibliography,
- Contributions of the ad-hoc group with stakeholders at JRC in Ispra to agree on the preparation of the report,
- VDI-Richtlinie bzgl. Flüssigmetallversprödung beim Verzinken.

All these valuable contributions are gratefully acknowledged.

The preparation of the report was accompanied by an ad-hoc group which met at JRC in Ispra on 19th of January 2009 and at CEN MC in Brussels on 26th of February.

Members of this ad-hoc group were:

M. Gérardin	Joint Research Centre of the European Commission (JRC)
A. Pinto	JRC
G. Tsionis	JRC
P. Özdemir	JRC
A. Da Costa	CEN-Management Centre
J. A. Calgaro	CEN/TC250 for Structural Eurocodes
F. Bijlaard	CEN/TC250/SC3 for EN 1993
G. Sedlacek	CEN/TC 250 (Convenor of the meeting)
R. Pope	CEN/TC135 for EN 1090
W. Smith	CEN/TC262 for EN 1461 and EN 14713
V. Bergmann	European Convention for Constructional Steel (ECCS) and Deutscher Stahlbau Verband (DSTV)
V. Hüller	Deutscher Ausschuß für Stahlbau (DAST)
B. Donnay	European Steel Producers/Arcelor Mittal
G. Axmann	European Steel Producers/Arcelor Mittal
M. Cook	European General Galvanizers Association (EGGA)
C. Leighfield	EGGA
A. Mohrenschildt	EGGA
M. Huckshold	Gemeinschaftsausschuss Verzinken (GAV)/EGGA
M. Feldmann	RWTH Aachen
D. Schäfer	RWTH Aachen

Thanks to all of them for their fruitful works and contributions

M. Feldmann

G. Sedlacek

Preface

- (1) Hot-dip-zinc-coating of steel components is an adequate measure for a reliable protection against corrosion of steel components that might impact durability and sustainability.
- (2) EN 1090, i.e. the standard for the delivery of prefabricated steel components and the execution of steel components and works, addresses zinc-coating. The EN-Standards for the zinc-coating process as EN ISO 1461 and EN ISO 14713 are also referred to in this code.
- (3) Cracking of steel under the corrosion attack by liquid zinc in the zinc bath has been observed since the 1930's and has been the concern of various research projects. The problem seemed to have been mastered for the usual design of components and the usual coating technology applied for many years.
- (4) Since 2000 with a peak in 2002, a more frequent occurrence of cracking and larger sizes of cracks that could impair the safety of structures could be observed. Cracking happened in particular after zinc-coated components had been assembled on site and cracks opened under loading filled or covered with zinc. These observations were coincident with the production of larger sizes of steel components characterized by larger plate thicknesses, the use of new constituent materials of higher strength, the use of new zinc alloys and the application of various dipping processes.
- (5) National and international research initiated for that purpose revealed that these cracks could be attributed to liquid metal embrittlement (LME) in the hot-zinc bath. The existing codes and standards and also some industry guidance established so far in some countries (e.g. in UK, Austria, Japan) do not give comprehensive provisions to prevent the risk of LME, so that in some countries initiatives came up to develop, on the basis of the existing research results, quantitative assessment rules that could mirror the effects of the various parameters on the phenomenon.
- (6) In view of the development of a consistent "European Standard Family", and the further harmonization of "National choices" in the single market for construction products and construction services there was the wish to channel these actions to achieve a common European procedure.
- (7) To this end representatives of the main stakeholders and parties concerned:
 - the European Commission represented by the Joint Research Centre in Ispra,
 - the CEN-Management Centre,
 - CEN/TC250 for the structural Eurocodes,
 - CEN/TC135 for the delivery of prefabricated steel components and the execution of components and works,
 - CEN/TC262 for zinc-coating process.

and also industrial representatives of the European steel producers (Arcelor Mittal), steel fabricators (ECCS), zinc coaters (EGGA), and also research institutes (RWTH Aachen) met in Ispra on 19th January 2009 to agree on the preparation of a “JRC-Scientific and Technical Report” on “Hot-dip-zinc-coating of prefabricated structural steel components”.

- (8) This report could be - in line with resolution No. 255 agreed at the CEN/TC250 meeting in Malta – a common basis for further CEN-actions in the various CEN-Technical Committees, and also serve in the meantime as a reference document for intermediate National actions.

Ispra, February 2010

J.A. Calgaro, F. Bijlaard, G. Sedlacek, CEN/TC250
R. Pope, CEN/TC135
W. Smith, CEN/TC262
M. Gérardin, A. Pinto, H. Varum, JRC

JRC-Scientific and Technical Report
Hot-dip-zinc-coating of prefabricated structural steel components

List of contents

Acknowledgements	1
Preface	3
List of contents	5
Executive Summary	7
1 Objective	9
2 Examples of cracks observed.....	11
3 Literature survey	13
4 Examination of macroscopic cracks	17
5 Conclusions for developing a quantitative assessment method to avoid cracking in the zinc bath	19
6 Standard test for determining the strain capacity of steels in the hot-zinc bath	21
7 Strain resistance of steel material from LNT-tests	25
8 Strain rate dependency from the LNT-test	31
9 Stress-strain requirements.....	35
9.1 General.....	35
9.2 Stationary strains from fabrication.....	35
9.3 Instationary strains from dipping	37
9.4 Superposition of stationary and instationary strains	38
9.5 Conclusions from variation of detail and plate thickness	38
10 Limit state assessments based on equivalent plastic strains.....	43
11 Validation of the strain-oriented assessment method.....	47
11.1 General	47
11.2 Structural components from car-parkings.....	47
11.3 Further prefabricated beams	48
11.4 Prefabricated columns	49
11.5 Latticed structures.....	50
11.6 Cold-formed components.....	51
11.7 Hollow section components	52
12 Transfer of results based on equivalent plastic strains into engineering models for practical assessments	53
13 Simplified engineering models for numerical assessment.....	55
14 Introduction of Confidence zones	63
15 Classification system without numerical assessment.....	67
16 Worked examples for using the classification method in section 15.....	73
16.1 General	73
16.2 Usual metal works.....	73
16.3 Detailed examples	75
16.4 Examples of choices made in the fabrication	79
17 Procedure tests.....	87
18 Supplementary rules for execution of hot-dip-zinc coating.....	89
18.1 General	89
18.2 Control of chemical composition of the zinc melt	89
18.2.1 Relevant Standards.....	89
18.2.2 Equipment, tools and sampling	89

18.2.3	Method for analysis	91
18.3	Non destructive testing procedures for zinc coated structural components ..	91
18.3.1	General	91
18.3.2	References to standards	91
18.3.3	Test personal	92
18.3.4	Preparation of surface for testing	92
18.3.5	Testing equipment and means for testing	92
18.3.6	Check of sufficient magnetizing of the testing system	92
18.3.7	Check of sufficient magnetizing for a project	92
18.3.8	Means for testing	92
18.3.9	Visual evaluation.....	93
18.3.10	Area to be tested	93
18.3.11	Limits for confidence.....	93
18.3.12	Demagnetizing.....	93
18.3.13	Treatment of structural components with faults	93
18.3.14	Documentation of the tests.....	95
19	Conclusion.....	97
20	Literature.....	99

**JRC-Scientific and Technical Report
Hot-dip-zinc-coating of prefabricated structural steel components**

Executive Summary

- (1) This JRC-Scientific and Technical Report gives information from pre-normative research methods to avoid liquid metal assisted cracking of prefabricated structural components during zinc-coating in the liquid zinc melt that may impair the structural safety of structures in which the components are built in.
- (2) This information provides a platform upon which further European design and product specifications can be developed. It may in particular affect the further developments of EN 1993, EN 1090 and EN ISO 1461 and EN ISO 14713.
- (3) This report gives the state of the art in understanding the mechanism of liquid metal assisted cracking in the zinc bath and methods and models that may be used to avoid it.
- (4) It could be a basis to propose rules for the design of steel components intended to be hot-dip-zinc-coated in such a way that the design is consistent with execution rules for hot-dip-zinc-coating.
- (5) The workability of the rules proposed for all metal works and steel works that are fabricated under EN 1090 and galvanized according to the rules in this report is demonstrated by worked examples.

1 Objective

- (1) This part of the JRC-Scientific and Technical Report deals with the phenomenon of “Liquid metal assisted cracking” (LMAC) of prefabricated steel components that may occur during hot-dip-zinc-coating in the hot-zinc bath and may in case of sufficient sizes of the cracks infringe the safety of the structures, which the steel components are built in.
- (2) Such serious cracks have been observed in particular after the year 2000, when the chemical composition of the zinc alloys was changed, the size of the components was increased and the material strength was enhanced.
- (3) Therefore, there is a need to inform on the cause of such cracks, to identify the most relevant parameters for cracking and to develop methods to avoid such cracking.
- (4) This information is a summary to give the state of the art on the issue. It is addressed to:
 1. the design of prefabricated steel components,
 2. the delivery of constituent products (semi-finished products) for the fabrication of steel components,
 3. the fabrication of steel components,
 4. the hot-dip-zinc-coating of steel components and subsequent checks.
- (5) Therefore this information provides a platform upon which further European design and product specifications can be developed. It may affect the further developments of:
 - EN 1993 for the preparation of the component specification (see EN 1090-1, 3.1.1 and 3.1.2),
 - hEN 1090-1 to cover galvanizing as for welding,
 - EN ISO 1461 and EN ISO 14713.

2 Examples of cracks observed

- (1) Figure 2-1 shows typical cases of cracking in prefabricated steel components that have been hot-dip-zinc-coated.

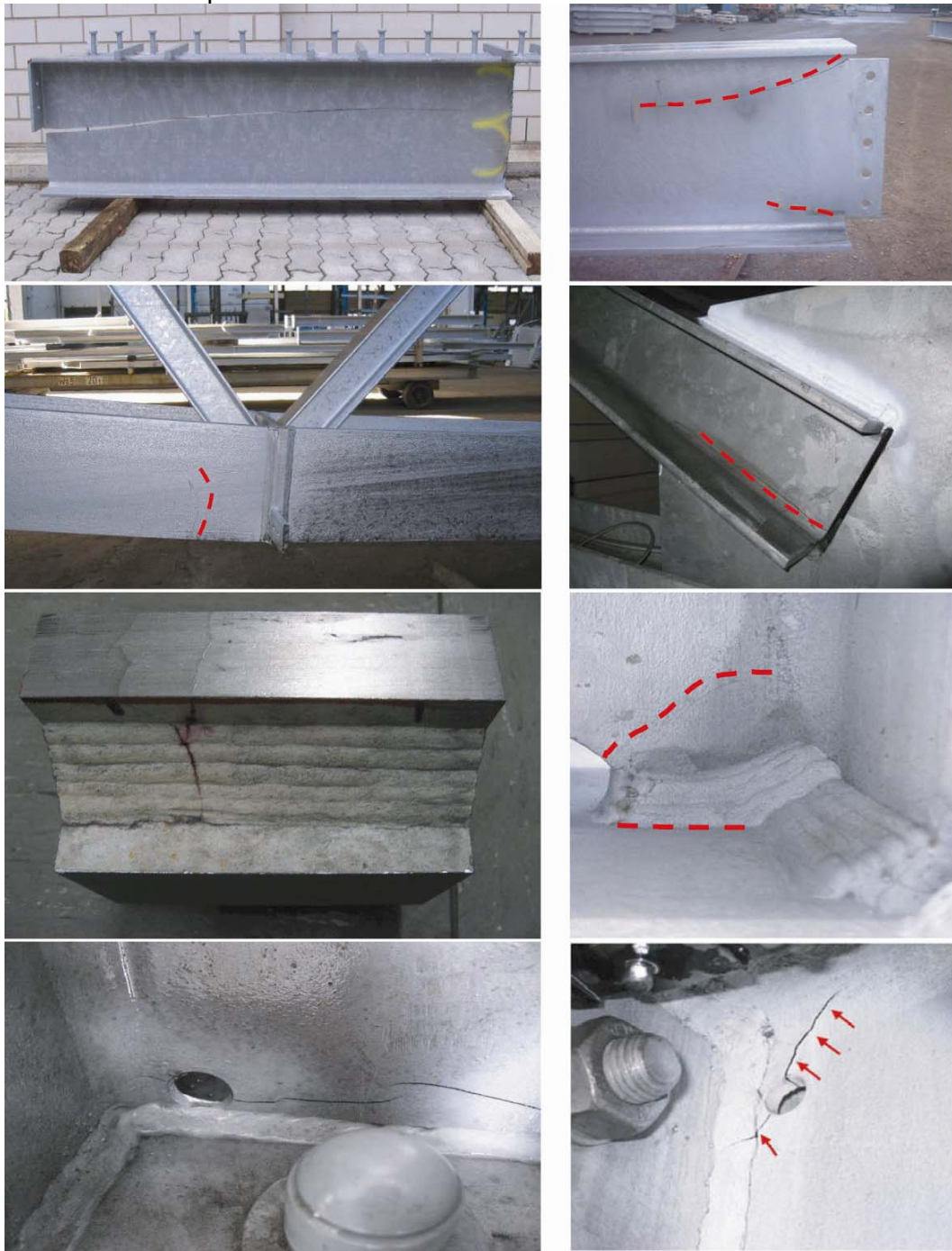


Fig. 2-1: Damages observed after zinc coating or after erection of hot-dip-zinc-coated structural components

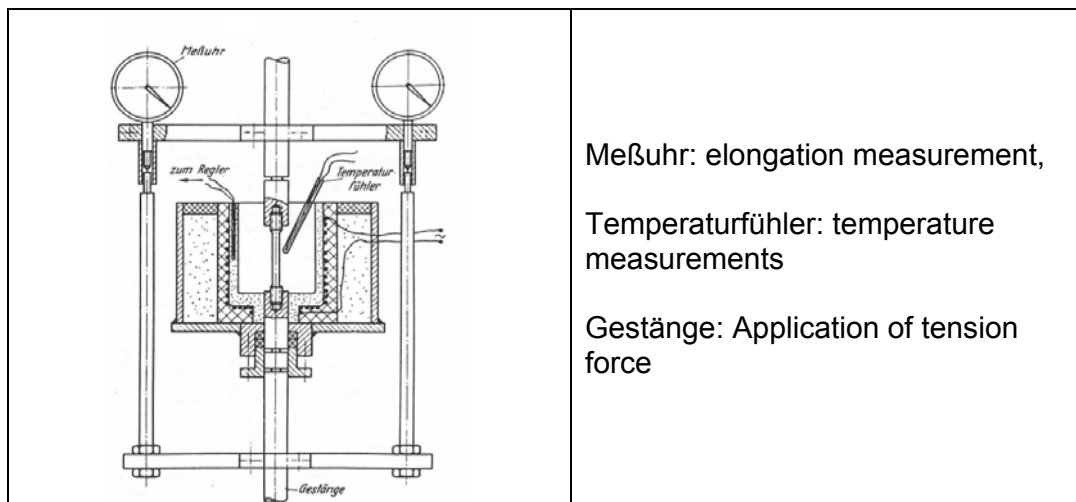
- (2) Particular spots in the components that are sensitive to cracking are e.g.:
- details at the end of steel beams with large depth, e.g. half end plates or flame cut or flame cut with subsequent grinding or drilled copes,

- the environment of welds in thick plates,
 - nodes of latticed structures, in particular those with hollow sections,
 - holes for the drainage of liquid zinc in corner areas.
- (3) Crack sizes may be some millimetres to some decimetres; all usual steel grades, e.g. S235, S355 and S460 have been affected by cracks.
 - (4) Cracks often are only detected after the steel components have been built in a structure and loaded, as the cracks in the steel components often are filled and covered with zinc. This also makes the detection of cracks after zinc-coating difficult and requires e.g. additional measures for magnet particle testing MT, as the usual application of EN 1290 would result in a reduced sensitivity for coat thicknesses $\geq 50 \mu\text{m}$.
 - (5) A peak in reports of cracking has occurred concerning work processed in the period 2000 to 2006. These reports are associated principally with the use of higher concentrations of tin (Sn) together with other elements in the zinc melt in a number of countries during this period, to obtain thinner coats that could be better controlled and would give better appearance of the surfaces.
 - (6) The information given below therefore relate to the analysis and investigations undertaken to find the causes of the crack damages most frequently observed that are related to Liquid Metal Embrittlement (LME) or Liquid Metal Assisted Cracking (LMAC) and result from a reduction of ultimate strain capacity of the steels in the hot-zinc bath.
 - (7) The phenomenon "Liquid metal embrittlement in the hot-zinc bath" is caused by the contact of steel with the liquid-zinc alloy that causes a reaction between the zinc-melt and the steel material (Fe-Zn-reaction). This reaction and its intensity is controlled by various parameters as the composition of the zinc alloy, the steel material, the local strains and the time of exposure as well as the strain resistance of the steel.
 - (8) Hydrogen induced cracking, that could be excluded as a cause for the cracking observed, is not dealt in this report. However, there may be cases where hydrogen induced cracking with subsequent liquid metal embrittlement may have been relevant.

3 Literature survey

(1) A literature survey for the period up to 2000 indicated that:

1. The phenomenon of Liquid Metal Embrittlement during hot-dip-zinc coating of steel has been dealt with since the 1930's:
 - Works on other materials than steels, e.g. for stress corrosion of aluminium alloys under attack of liquid metals as Mercury, Lithium, Gallium, Tin, Zinc, Lead had already revealed the importance of
 - the chemical-physical affinity of the liquid metal with limited solubility in the base metal,
 - the formation of eutectica with low solution temperature in case of liquid metal alloys.
 - Early works on steel materials were mainly related to specific questions of the durability of the kettles holding the zinc melt. Though the evaluation of such test-reports is difficult because of lack of suitable data in the documentations, some of the conclusions could be drawn as follows [25-27]:
 - a) Tests with steel specimen in tension in the liquid zinc bath, see [fig. 3-1](#) reveal a dependence between the stress-level, geometrical notch situation and time to fracture see for example [fig. 3-2](#),
 - b) The frozen zinc layer forming in the beginning of dipping is torn by temperature induced strains and leads to further exposure of steel surfaces to liquid zinc thus explaining the time effect of exposure.
 - c) There are dependences between the time to fracture and the strain rate $\dot{\epsilon}$ applied to the steel components: the smaller the strain rate, the greater the time to fracture.



Meßuhr: elongation measurement,

Temperaturfühler: temperature measurements

Gestänge: Application of tension force

Fig. 3-1 Test set-up [26]

steel	Shape of specimen	stress [N/mm ²]	Time to fracture
TU St 37	„unnotched“	250	6 min
	„notched“	330	70 s
MR St 60	„unnotched“	510	5 min
	„notched“	400	3,5 min

Fig. 3-2: Test results [26]

Unfortunately these investigations on the Liquid Metal Embrittlement for hot-dip-zinc-coating were not continuous and not systematic, so that only the qualitative influence of stress, strain, exposure time, zinc alloy and steel quality have been detected however without giving quantitative data suitable for assessments.

- Japanese investigations in the 1980's revealed for the first time the influence of the effects of external loading of steel and the reduced resistance of steel to the loading in the zinc bath:

- Fig. 3-3 gives stress-strain curves of steel specimens for steels intended to be used for masts and towers that reveal that the strain capacity of the steel in the molten zinc can be reduced significantly.

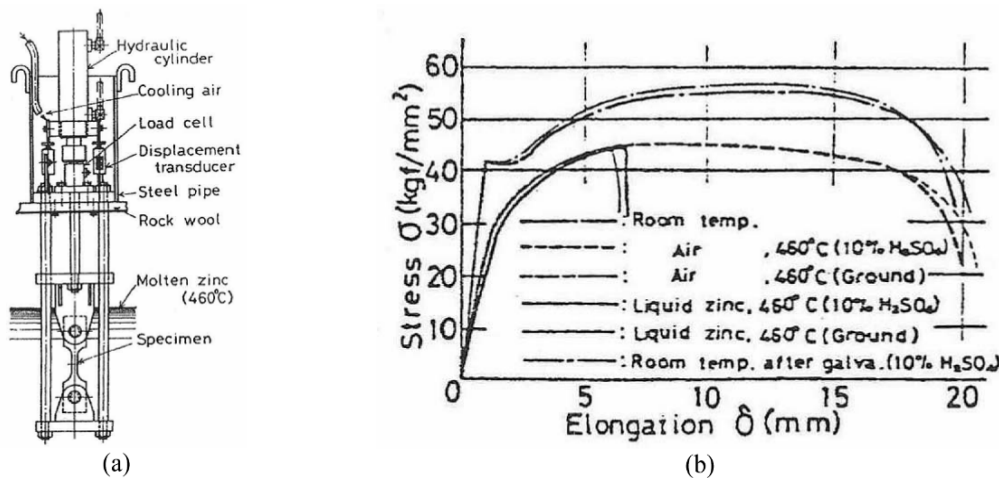


Fig. 3-3: Determination of stress-elongation curves for steel in the liquid zinc bath [36, 37] a) Testing set-up, b) stress-elongation curves

- Further tests to clarify the effects of the steel composition and fabrication on the fracture in the molten zinc lead to a "susceptibility factor" s_{LM400} :

$$s_{LM400} = \frac{\text{notched bar fracture stress in molten zinc}}{\text{notched bar fracture stress without any zinc}} \cdot 100\% \quad (3.1)$$

where the index 400 indicates that the fracture strength has been determined after an exposure time of 400 sec. Recommendations have been given in Japan to reduce this susceptibility factor to avoid cracking in the zinc bath. However, the susceptibility index proved to be not suitable to explain the damages that occurred after the year 2000 as noted in section 2.

- Japanese investigations have also been made to identify the stress-strain-development during dipping of steel components in the hot zinc bath.

Fig. 3-4 gives an example for the influence of the dipping speed on the stress-intensity factor K of a plate with a crack. This shows that a low dipping speed effects an increase of K -requirement.

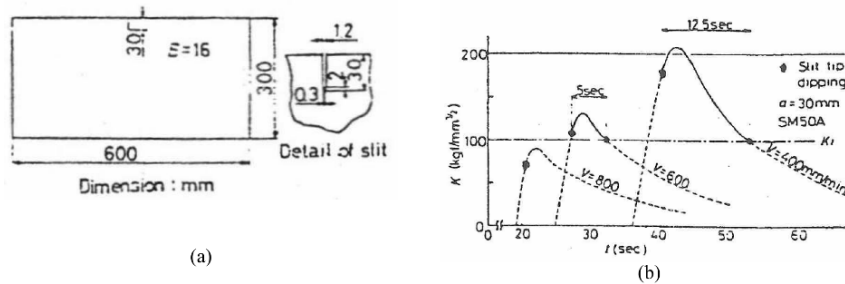


Fig. 3-4: Dependence of stress intensity factor K in dipping situation with different dipping speeds a) test specimen, b) influence of dipping speed

Also large scale tests with hollow sections for masts and towers were carried out to determine the development of stresses and strains during the dipping process, fig. 3-5.

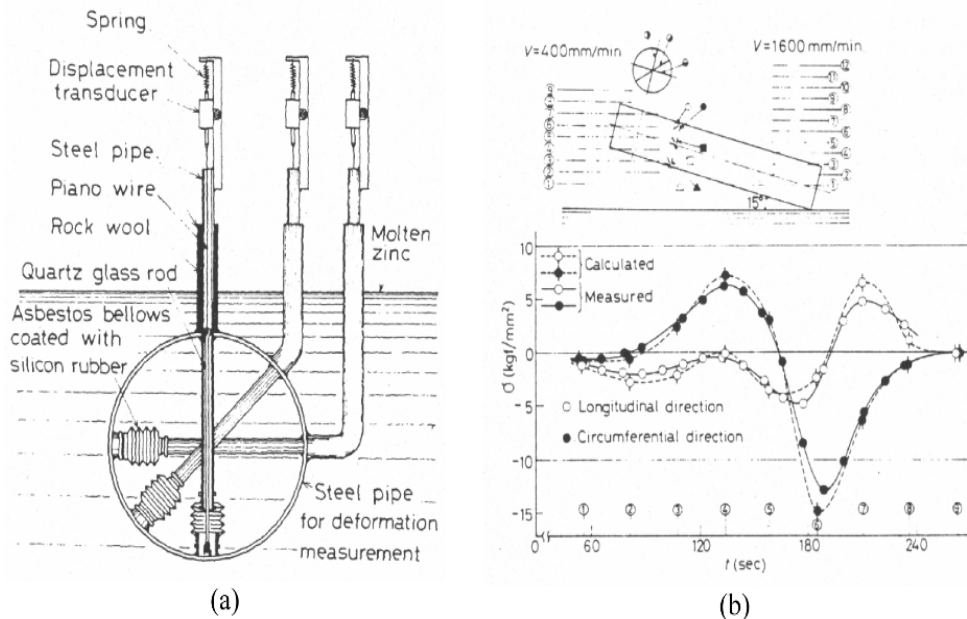


Fig. 3-5: Large scale tests for hollow sections for masts and towers a) measuring devices, b) measured and calculated time history of stresses during dipping ($v = 0.4$ m/min) [43]

These tests demonstrate:

- the development of stresses with characteristic alternating sign during the dipping process,
- the dependence of the maximum strain requirement on the dipping speed; the smaller the dipping speed the higher the strain occurring to be regarded as strain requirement.

3. In conclusion, the works documented in literature until the year 2000 give valuable information, mainly qualitatively or related to specific cases, so that the basis of a quantitative assessment to avoid liquid metal induced cracking in the zinc bath had not yet been developed at that time.

They give however already all key information necessary to identify the direction of further research that has been carried out after the year 2000 to establish the basis for methods for such quantitative assessment.

4 Examination of macroscopic cracks

- (1) Fig. 4-1 to fig. 4-4 give some microscopic views of cracks in the web of a I-profile made of S355J2G3 that occurred in a zinc melt with a Tin (Sn) content of 1 % and a lead (Pb) content of about 1 %.

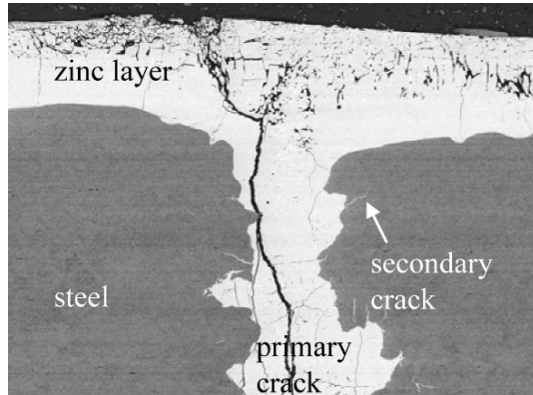


Fig. 4-1: Primary crack and secondary crack (200x)

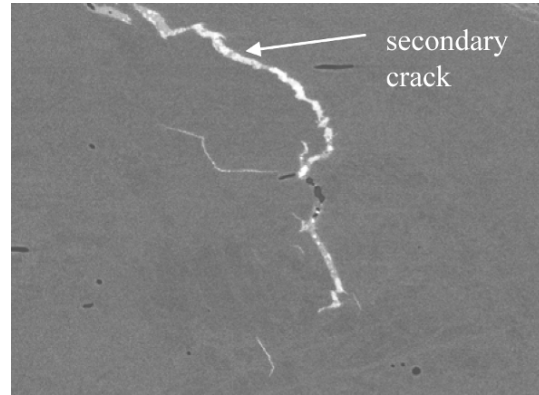


Fig. 4-2: Secondary crack (2000x)

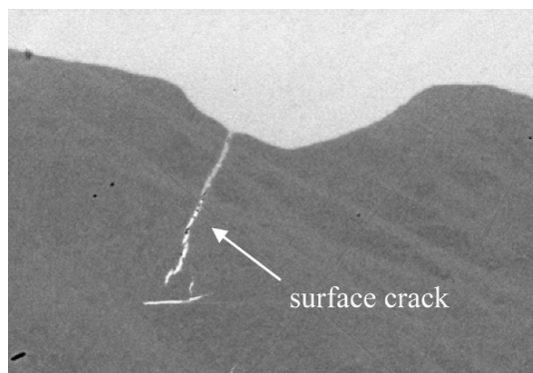


Fig. 4-3: Surface crack starting from dimple (2000x)

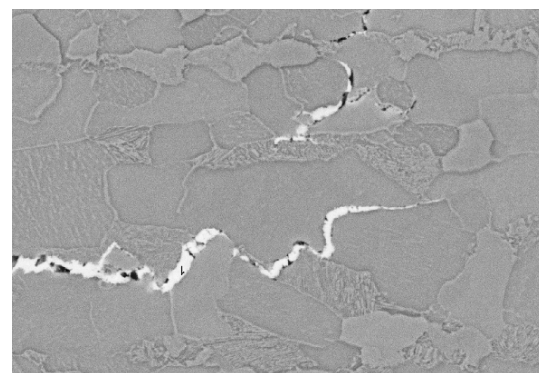


Fig. 4-4: Intergranular crack in ferrite-pearlite structure (5000x)

- (2) The figures show the following:

1. There are primary wide macro-cracks starting at the steel surface with narrow secondary cracks the size of which is either limited to the surface or going through the depth of the plate. The cracks are filled with components of the zinc melt. Fig. 4-4 shows that the cracks are intercrystalline.
2. In the secondary crack and the crack tips of the primary cracks (with small widths) a decomposition and segregation of the alloy additives as Sn, Pb and Bi has taken place, whereas the wide primary cracks are filled with an alloy comparable with the composition of the regular zinc bath.
3. There is a roughening effect of the additives as Sn on the surface of the steel.

- (3) The phenomena illustrated in fig. 4-1 to 4-4 are typical for liquid metal embrittlement, where a liquid metal phase, consisting of the components Fe, Zn and Sn or others penetrates into a solid metal, here steel, via the grain-borders.
- (4) The physical mechanism for this is that the cohesion force between the grain borders of the steel is smaller than the adhesion force of the liquid metal phase to the surface of the steel grains; hence the Gibbs-energy is reduced by the embrittlement.

5 Conclusions for developing a quantitative assessment method to avoid cracking in the zinc bath

(1) From former investigations on LME performed in various countries and the thorough examination of the cracks, the following conclusions could be drawn for the development of a quantitative assessment method to avoid cracking in the zinc bath:

1. Apparently the effect of liquid metal embrittlement of steel in the hot-zinc alloy is a reduction of the ultimate strain capacity that should be quantified by a “standard test” that simulates the realistic behaviour of steel components in the zinc bath.

Such a test should give numerical results for a “strain resistance” ε_R depending on several parameters that should be evaluated according to EN 1990-Annex D to obtain “characteristic resistance” values.

2. The “characteristic resistance” should be given for two design situations:
 - a) non-stationary or dipping phase: a design situation during the dipping process when the strain requirements from non-stationary strains from the temperature differences (superimposed on stationary strains from the steel manufacturing process (rolling and straightening of the semi-finished product) and fabrication of the steel components (welding, bending, cutting, punching etc.)) are a maximum,
 - b) stationary or holding phase: a design situation after the full heating of the steel component in the zinc bath, when the non-stationary strains have died down, however the strain capacity of the steel is further diminished due to the long exposure time (holding time).

3. The strain requirements ε_E that could be used for a limit state assessment

$$\varepsilon_E \leq \varepsilon_R \quad (5.1)$$

should also be given as characteristic values and be determined by numerical simulations of the fabrication procedures and the dipping and holding process.

In consequence, both for the instationary design situation (dipping process) and for the stationary design situation (holding phase) the limit state equations read

$$\varepsilon_{Ed} \leq \varepsilon_{Rd} \quad (5.2)$$

where the index d designates “design values”, that are derived from “characteristic values” to obtain the required reliability.

4. This strain-oriented procedure is consistent with the assumptions made in modern “damage theory” that applies in the upper-shelf region of the

temperature-toughness diagram for ferrite steels. This theory is capable to simulate fracture-mechanics tests as well as the fracture behaviour of steels in monotonic and cyclic loading in the elastic and plastic range and also works with “equivalent plastic strains”.

6 Standard test for determining the strain capacity of steels in the hot-zinc bath

- (1) The “standard test“ shall provide characteristic values of “equivalent plastic strain”-resistance in the zinc melt, that depends on the various process parameters, such as:
 - composition of zinc melt and bath temperature,
 - steel quality,
 - microstructure and surface condition of steel product or of machined surfaces,
 - strain rate.
- (2) The standard test needs sufficiently small test specimens, however the results should be independent on the scale and the particular loading condition of the test specimen and should be transferrable to any large scale structural component.
- (3) Such a test has been developed from the fracture mechanics CT-test specimen: the LNT test specimen.

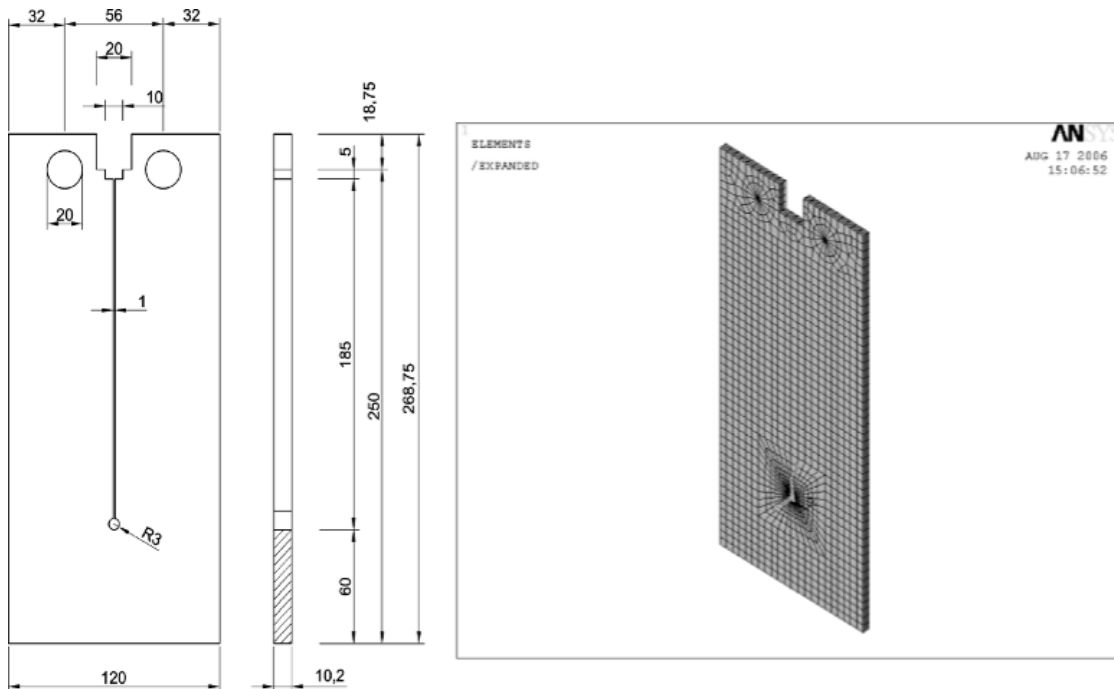


Fig. 6-1: LNT-test specimen and FEM-mesh for numerical simulation of test

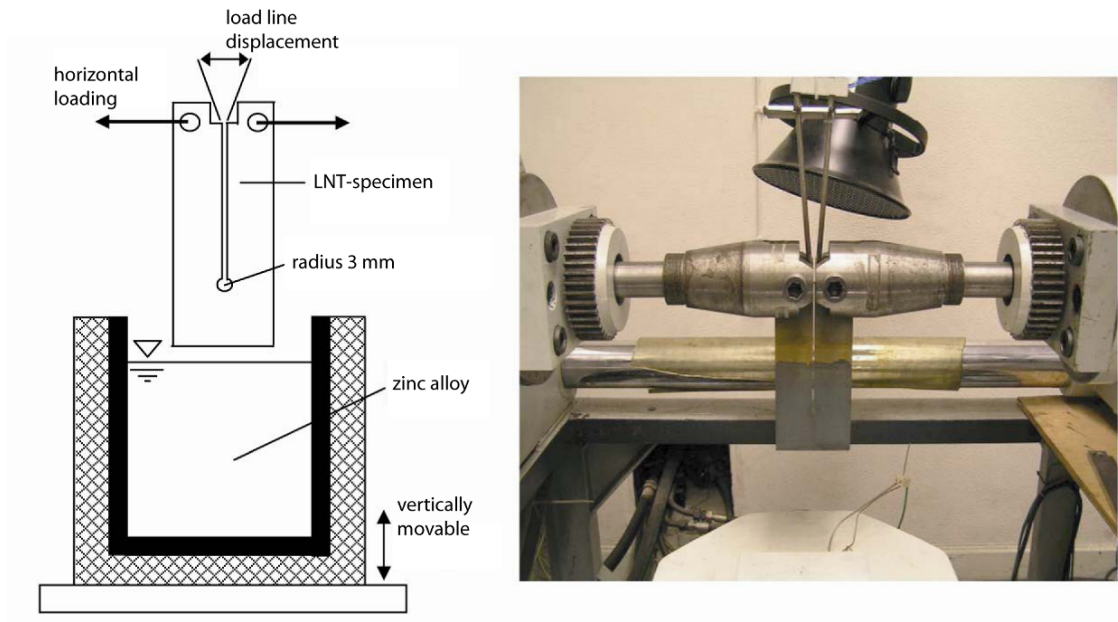


Fig. 6-2: LNT-test setup and load application

- (4) Fig. 6-1 gives details of the LNT-test specimen with its dimensions in mm. It can be dipped into the zinc melt and loaded horizontally by tensile forces with varying force-time characteristics, see fig. 6-2.
- (5) The sharp crack tip of the CT-test specimen (in general obtained by applying fatigue load cycles to these test specimens) is substituted by a drilled hole, the bottom of which is locally strained by the tension forces applied at the top of the specimen in such a way, that after a certain exposure time cracking at this hot-spot can be expected.

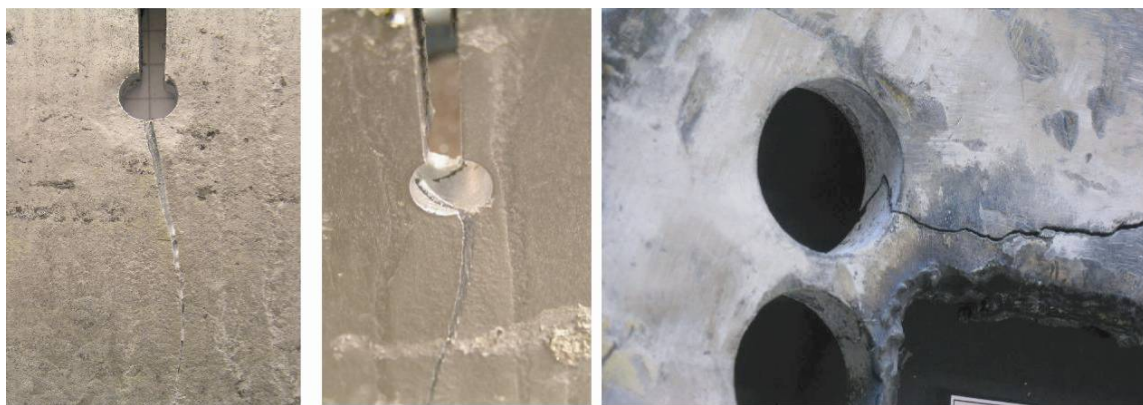


Fig. 6-3: Cracks at bottom of hole observed in tests and cracks observed in practice

- (6) Fig. 6-3 gives the cracks observed in the test and cracks observed in practice at a prefabricated steel component.
- (7) The local equivalent plastic strain at the bottom of the hole affected by the tensile forces can be determined by FEM calculations

$$\varepsilon_{pl,v} = \int \sqrt{\frac{2}{3} \dot{\varepsilon}_{pl} \dot{\varepsilon}_{pl}} dt \quad (6.1)$$

- (8) Fig. 6-4 gives an example of such calculations with the finite element mesh adopted (Fig. 6-4a) and the plot of the plastic strains (Fig. 6-4b).

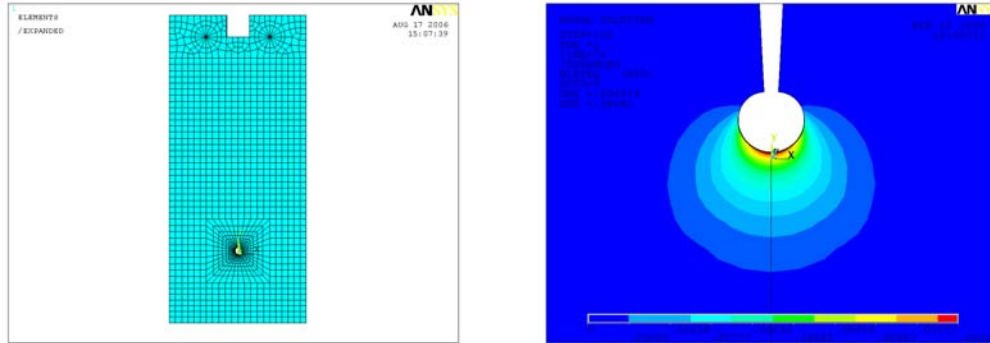


Fig. 6-4: FE-mesh and plot of equivalent plastic strains

- (9) Fig. 6-5 gives the relationship between the displacement in the line of load application and the local equivalent plastic strain resulting from the loads.

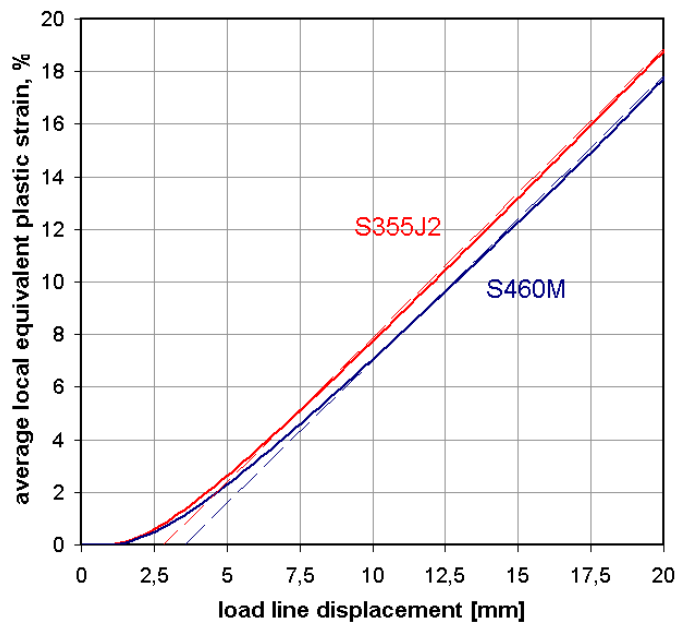


Fig. 6-5: Master-curves for the determination of ε_{pl}

7 Strain resistance of steel material from LNT-tests

- (1) As indicated in Fig. 6-5 the load-displacement curve in the line of load application can be measured in the test. It exhibits a sudden drop when cracking relevant for structural assessment starts.
- (2) FEM-calculations can give both the numerical simulation of the load displacement curve and the associated local equivalent plastic strain at the bottom of the hole where the start of the crack growth is expected.

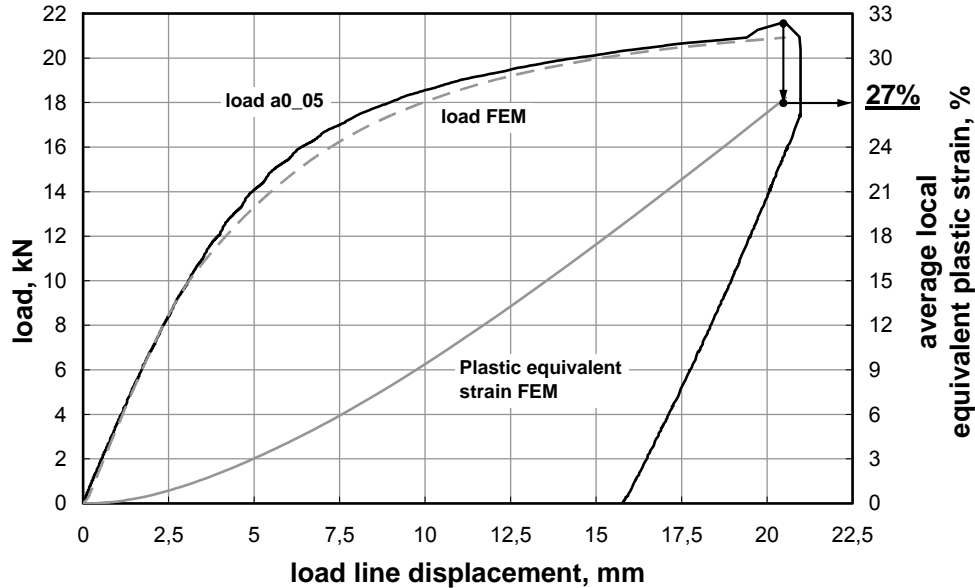


Fig. 7-1: Load displacement and equivalent plastic strain displacement curve for steel exposed to the air with a temperature of 450 °C

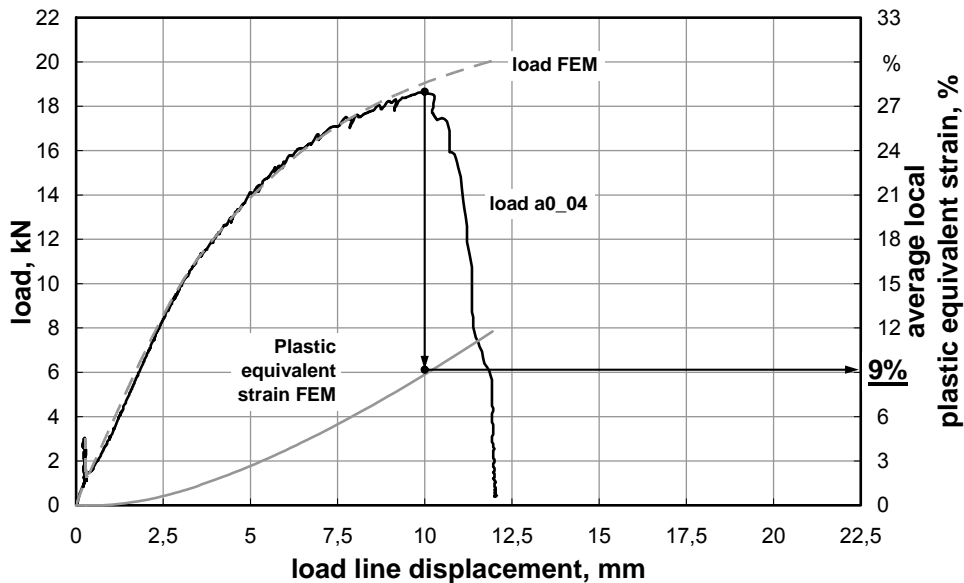


Fig. 7-2: Load displacement and equivalent plastic strain displacement curve in liquid zinc alloy with Sn 1,2%

- (3) Tests are run with a strain rate $\dot{\epsilon} \approx 5 \cdot 10^{-4}$ to simulate the design situation during dipping into the zinc bath with instationary stresses and strains.
- (4) While the load-displacement curve in [fig. 7-1](#) applies for a test specimen heated to 450°C without the corrosion effect of the liquid zinc bath (test specimen exposed to the air), giving the plastic strain capacity of 27 %, [fig. 7-2](#) gives the values for the zinc alloy a0 with a tin (Sn) content of 1,2 %, see [fig. 7-3](#). All data are related to steel S460.

alloy	Pb, M.-%	Sn, M.-%	Bi, M.-%	Al, M.-%	Ni, M.-%	Fe, M.-%
a0	---	1,20	0,11	0,0057	0,047	0,028
a1	0,70	---	---	0,005	---	0,03
a2	1,00	1,1	0,05	0,005	0,05	0,03

Fig. 7-3: Chemical composition of zinc alloys used for tests (the composition of alloy a2 does not comply with EN ISO 1461 (sum of other elements $\leq 2,0\%$))

- (5) A comparison of test results and the associated scatter of data is given in [fig. 7-4](#).

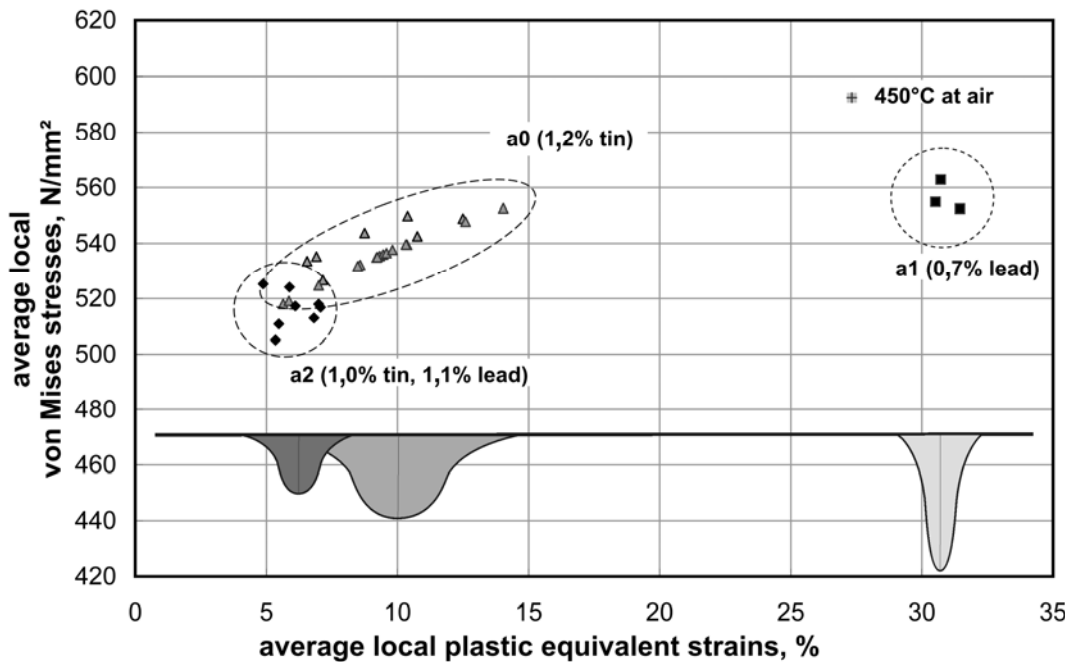


Fig. 7-4: Test results of LNT-rests

- (6) A systematic investigation of the influence of the components Tin (Sn), Lead (Pb) and Bismuth (Bi) in the zinc alloy [71, 72] has lead to the equivalent plastic strain resistances $\epsilon_{pl,c}$ [%] as given for the example of Tin in [fig. 7-5](#) and Tin and Lead in [fig. 7-6](#). This investigation demonstrates that:

1. Sn is the relevant constituent that gives the steepest gradient for results,

2. Classes for differentiation of resistances can be established with the Sn-content being the leading parameter and the contents of other constituents being limited:

- class 1 $\text{Sn} \leq 0,1 \%$
- class 2 $0,1 \% < \text{Sn} \leq 0,3 \%$
- class 3 $0,3 \% < \text{Sn}$

where the class-number signifies increasing aggressiveness, see [fig. 7-5](#).

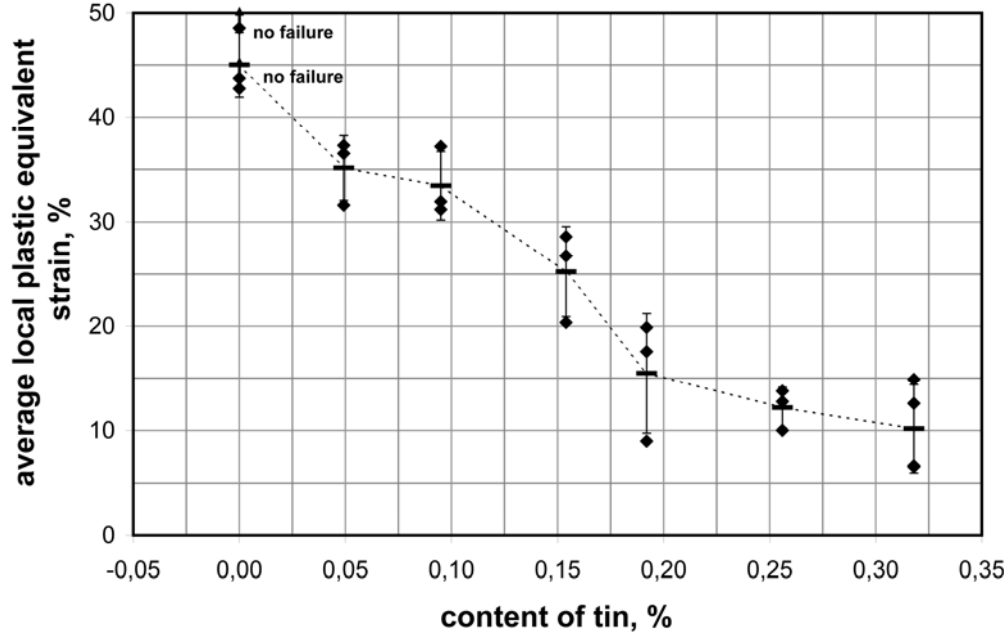


Fig. 7-5: Influence of Sn on equivalent plastic strain resistance

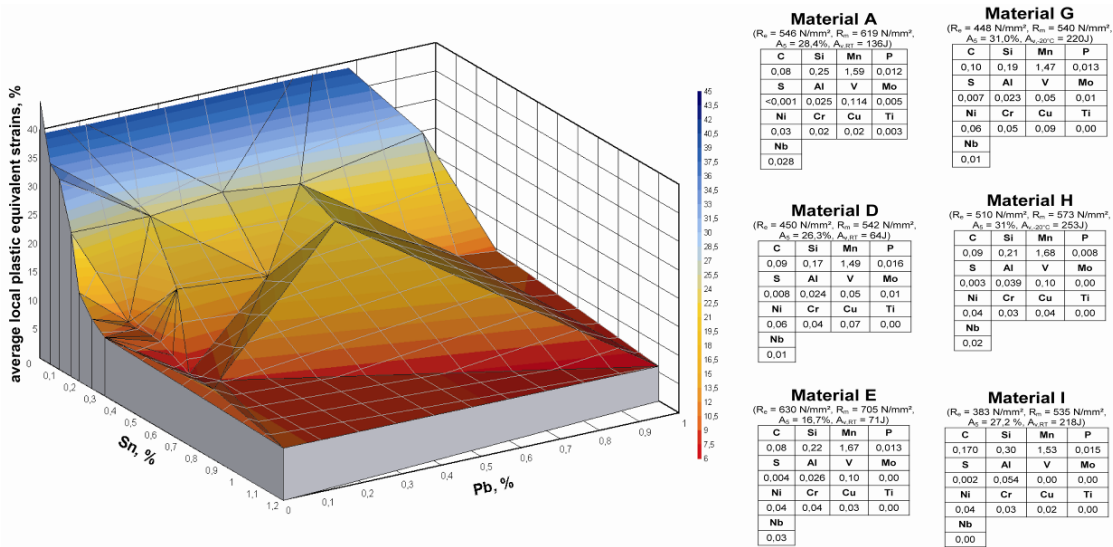


Fig. 7-6: Influence of interaction of Sn and Pb on equivalent plastic strain resistance based on mean values

- (7) Fig. 7-7 gives a suitable classification of zinc alloys in which also the contents of Pb and Bi are limited to $Pb + 10Bi < 1,5\%$ [75]. Fig. 7-7 gives also the relevant plastic strain resistances $\varepsilon_{R,ref}$, taking account the scatter of results.

Note: The limitation of strain resistance only applies in the hot zinc melt. After galvanizing the strain resistance of the steel is recovered.

- (8) A side effect of the LNT-test is that the heat transfer coefficient α_t from zinc to steel which is required to calculate the time for heating the steel component from the temperature before dipping to the temperature of the zinc bath can be experimentally determined.

Zinc alloy class	Weight proportion of zinc alloy					Plastic strain resistance $\varepsilon_{R,ref}$	Effective heat transfer coefficient $\alpha_{t,eff}$
	Sn	Pb + 10 Bi	Ni	Al	Sum of other elements (without Zn + Fe)		
1	Sn \leq 0,1%	1,5 %	< 0,1%	< 0,1%	< 0,1%	12%	3000 W/m ² K
2	0,1% < Sn \leq 0,3%	1,5 %	< 0,1%	< 0,1%	< 0,1%	6%	6000 W/m ² K
3	Sn > 0,3%	1,3 %	< 0,1%	< 0,1%	< 0,1%	2%	15000 W/m ² K

Fig. 7-7: Equivalent plastic strain resistances measured for double salt flux with a salt content of flux ≥ 450 g/l and iron content in flux < 10 g/l. The values $\alpha_{t,eff}$ apply to this type of flux and LNT-specimen and have to be adapted to large scale components

Alternative fluxes may have other concentrations that may give different values of $\alpha_{t,eff}$.

- (9) Fig. 7-8 gives a comparison of the temperature-time curve as measured during dipping and as calculated with a numerical value using α_t . The values α_t relevant for the different zinc alloy classes also are given in Fig. 7-7.

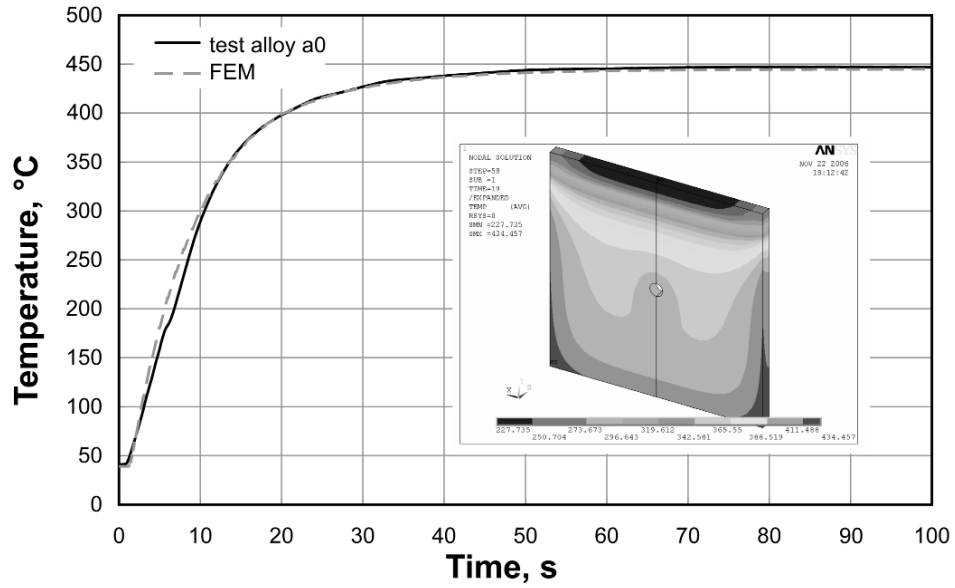


Fig. 7-8: Comparison of the time histories of temperature of a specimen as measured and as calculated

8 Strain rate dependency from the LNT-test

- (1) The LNT-tests is deformation-controlled with a proportionality between the displacement δ and the plastic strain ε at the bottom of the hole, see [fig. 8-1](#).

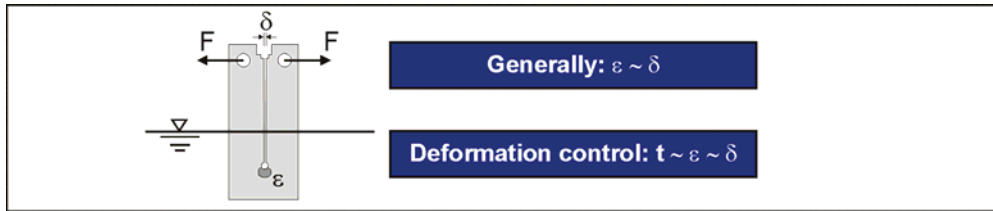


Fig. 8-1: Relation of time, load-line deformation and strain at notch tip for deformation controlled LNT-tests

- (2) Tests were carried out for a matrix of parameters, with variation of the strain rate $\dot{\varepsilon}$ for a given alloy and of the alloys for a given strain rate where the corrosion aggressiveness decreased with the number of alloy, see [fig. 8-2](#).
- (3) The damaging effect of the alloy is expressed by the integral $A = \int \varepsilon_{pl}(t) dt$ (area under the $\varepsilon_{pl}(t)$ -curve) see [fig. 8-3](#). [Fig. 8-4](#) shows typical curves for the dependency of strain rate, where the integral A is plotted in the logarithmic scale $\ln A$.

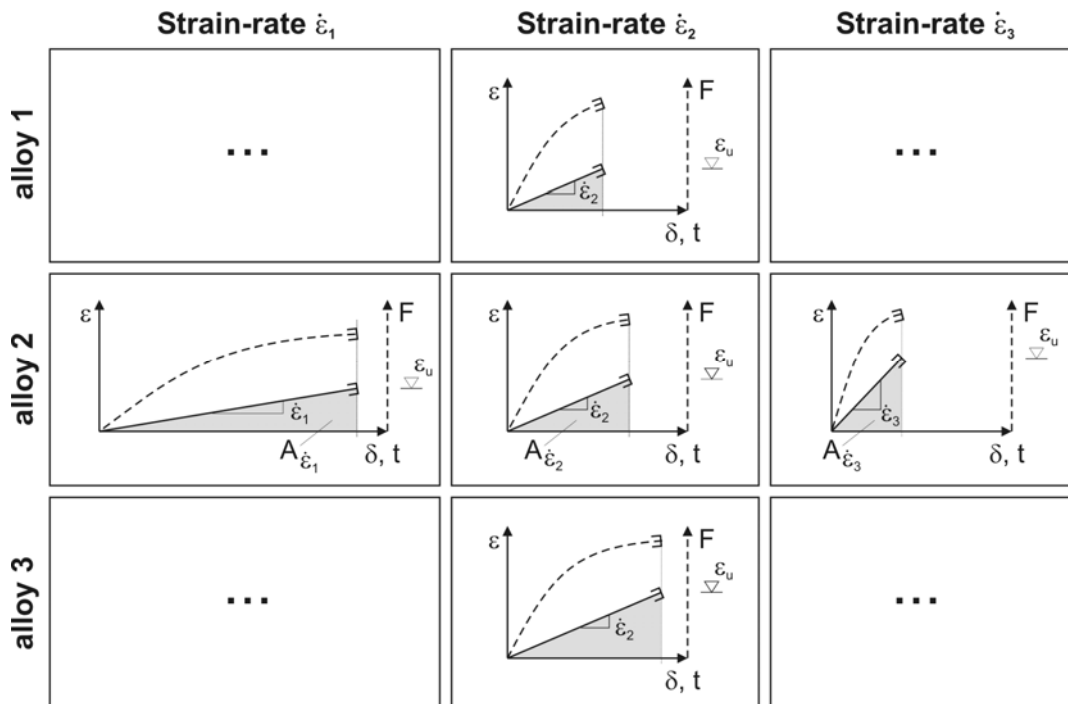


Fig. 8-2: Dependence of the LNT-test results on the variation of zinc alloy and variation of the strain rate as used for tests

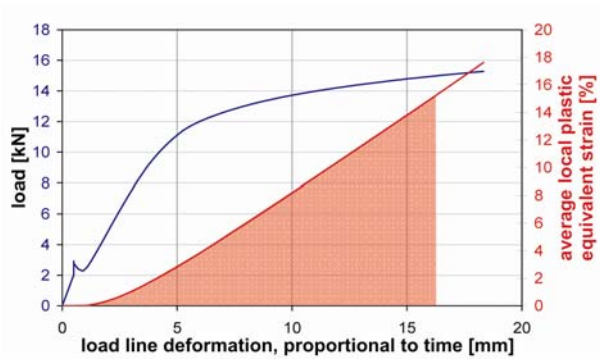
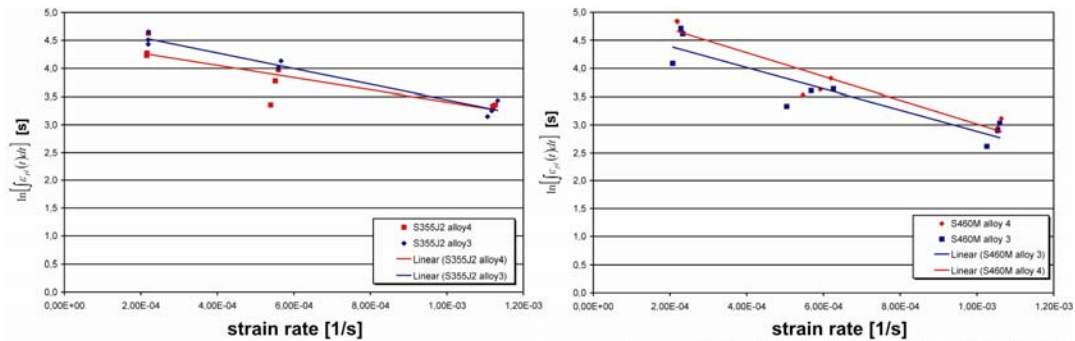


Fig. 8-3: Damage effect expressed by the integral $A = \int \varepsilon_{pl}(t) dt$



	Pb. M.-%	Sn. M.-%	Bi. M.-%	Al. M.-%	Ni. M.-%	Fe. M.-%
alloy 3	0,90	0,3	0,09	0,005	---	0,02
alloy 4	1,00	0,3	0,08	0,002	---	0,04

Fig. 8-4: Typical curves $\ln A$ for damage A versus strain rate $\dot{\varepsilon}$

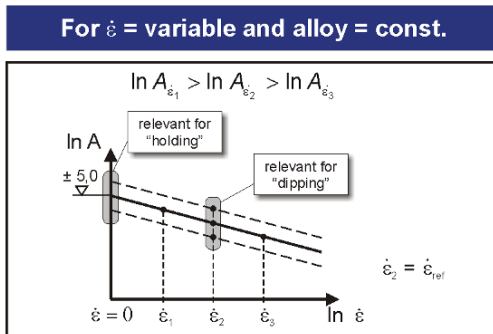
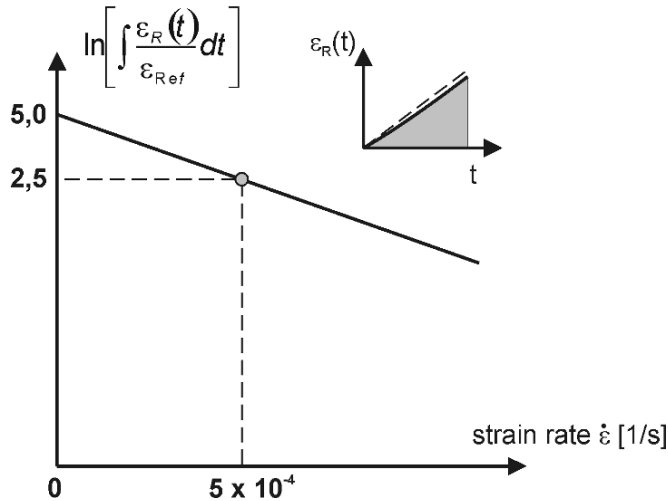


Fig. 8-5: Linear model for the $A-\dot{\varepsilon}$ curve in double logarithmic scale


 Fig. 8-6: Correlation related to $\dot{\varepsilon}$

- (4) The conclusion from the tests can be taken from [fig. 8-5](#), where a linear model in the double logarithmic scale for A and $\dot{\varepsilon}$ is given and typical strain rates for “dipping” ($\dot{\varepsilon}_2 = \dot{\varepsilon}_{ref}$ for the relevant strain capacities ε_{ref} in [fig. 7-6](#)) and for “holding” ($\dot{\varepsilon} = 0$) are indicated. As [fig. 8-3](#) and [fig. 8-4](#) show, a decrease of the strain rate from test to test while leaving the composition of the zinc alloy constant leads to lower strain resistances.
- (5) In using the basic equation in [fig. 8-6](#), where the related value

$$\ln \bar{A} = \ln \left[\int \frac{\varepsilon_R(t)}{\varepsilon_{ref}} dt \right] \quad (8.1)$$

versus the strain rate $\dot{\varepsilon} [1/s]$ is plotted and the typical “dipping” situation can be expressed by the pair

$$\dot{\varepsilon}_{R,ref} = 5 \cdot 10^{-4} \text{ and } \ln \bar{A} = 2,5 \quad (8.2)$$

and the “holding” situation by the pair

$$\dot{\varepsilon}_R = 0 \text{ and } \ln \bar{A} = 5,0, \quad (8.3)$$

the following conclusion can be drawn for the holding time t_s

$$\int_0^{t_s} \frac{\varepsilon(t) dt}{\varepsilon_{R,ref}} = e^5. \quad (8.4)$$

With using a linear function for the $\varepsilon(t)$ curve, see [fig. 8-6](#):

$$\int_0^{\varepsilon_R(t_S)} \frac{\varepsilon(t)}{\varepsilon_{R,ref}^*} dt \approx 0,5 \frac{\varepsilon_R(t_S)}{\varepsilon_{R,ref}^*} \cdot t_S \quad (8.5)$$

the holding time reads

$$t_S = 2.148 \frac{\varepsilon_{R,ref}^*}{\varepsilon_R(t_S)} [s] = \frac{5\varepsilon_{R,ref}^*}{\varepsilon_R(t_S)} [\text{min}] \quad (8.6)$$

- (6) In using $\varepsilon_{R,ref}^* = 60 \varepsilon_{R,ref}$ the critical holding time t_S for various zinc alloys can be determined as given in fig. 8-7.

Strain requirement ε_{ES}	Zinc class		
	1	2	3
	$\varepsilon_{R,ref} = 12 \%$	$\varepsilon_{R,ref} = 6 \%$	$\varepsilon_{R,ref} = 2 \%$
0,5 %	120 min.	60 min.	20 min.
1,0 %	60 min.	30 min.	10 min.
1,5 %	40 min.	20 min.	6,7 min.
2,0 %	30 min.	15 min.	5 min.

Fig. 8-7: Critical dipping time t_s for various zinc alloy classes and strain requirements ($\varepsilon_{Ref} = \varepsilon^*/60$)

- (7) It is evident from fig. 8-7 that for zinc alloy class 1 and all relevant strain requirements ε_{ES} all time values t_s for holding are within suitable limits, whereas zinc alloy classes 2 and 3 require restrictions of holding time.

9 Stress-strain requirements

9.1 General

- (1) Equivalent plastic strain requirements result from an accumulation of strains due to:
1. time history of fabrication,
 2. time history of heating process during dipping if the instationary heating process is relevant for cracking,
 3. time history of the exposure in the zinc bath, if the time effect on the reduction of strain capacity (holding time) is relevant for cracking.

9.2 Stationary strains from fabrication

- (1) An example for the effects of fabrication on strain requirements is given in [fig. 9-1](#). This figure shows a typical stationary stress/strain distribution in rolled profiles, where due to different speeds of cooling down from the rolling heat the massive flanges get residual tension and the webs get residual compression. These stress/strain distributions are constant along the length of the beam except at their ends where equilibrium between the tensile and the compressive areas of the beam is effected by forming a tensile arch which causes transverse tensile stresses in parallel to the cut surfaces at the beam ends.

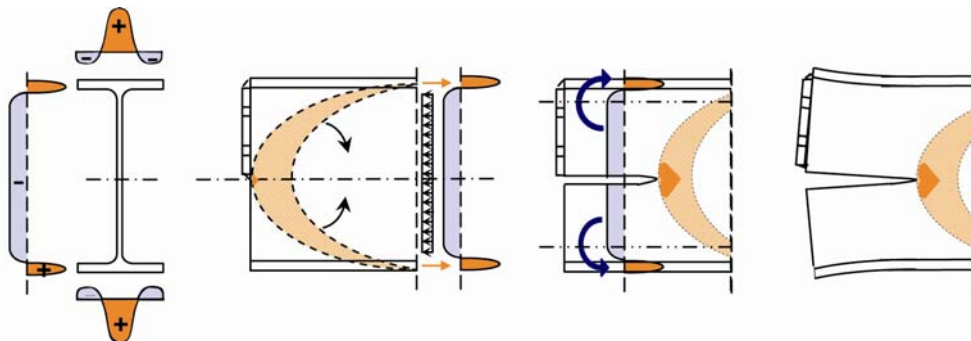


Fig. 9-1: Stress/strain distribution from the rolling of beams and crack propagation due to the crack-driving effect of the moving tensile arch at beam ends

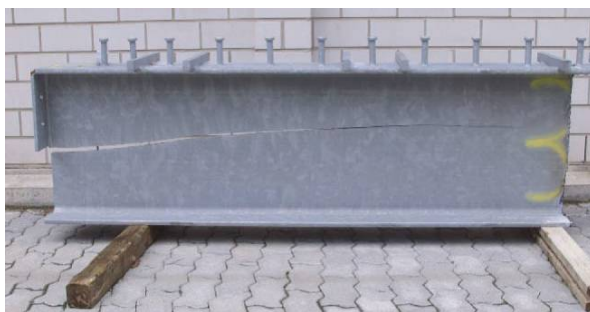


Fig. 9-2: Example for a large crack formed at the ends of a 16 m long beam for a composite floor detected after galvanizing

- (2) If at this surface strain concentrations are present due to welding and shape effects and additional plastic strains form due to the temperature gradient from dipping into the zinc bath a liquid metal assisted macro crack may occur that propagates to a large size due to the crack-driving effect of the accompanying tensile arch, see [fig. 9-2](#).
- (3) A particular hazard results from cold forming of prefabricated structural components, e.g. for hooks, loops etc., where liquid metal assisted cracking starts at the concave side of the imposed curvature.
- (4) [Fig. 9-3](#) gives an example of a floor beam that was precambered before hot dip galvanizing by polygonal cold forming with three point plastic bending. At the points of transverse load introduction to the bottom flange plastic prints of the tool with large local plastic deformations at the flange surface took place that were superimposed with tensile stresses from the elastic reactions of the beam to the plastification of the cross-section, see [fig. 9-4](#). After concreting of the floor deck, the beam collapsed by opening of a liquid metal assisted crack filled with zinc.

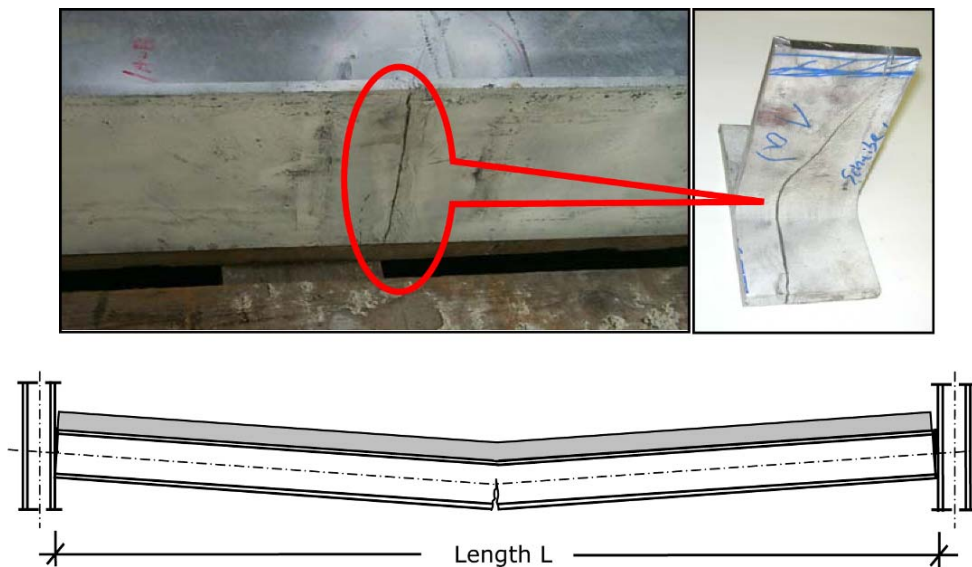


Figure 9-3: Opening of liquid metal induced crack at a bottom chord of a floor beam observed after concreting of the floor deck

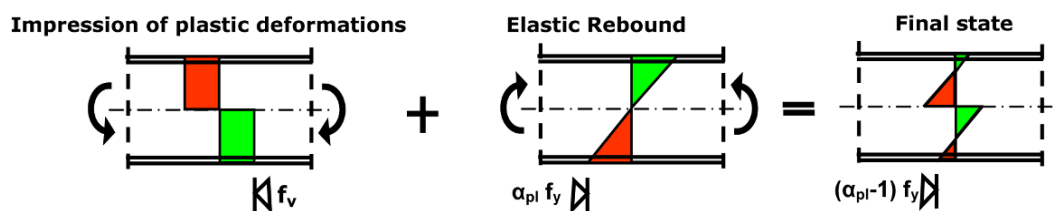


Figure 9-4: Stress blocks from plastic cold forming and elastic stresses from reactions of the beam to cold forming that give residual tensile stresses to the bottom flange on the concave side of the precambered beam

9.3 Instationary strains from dipping

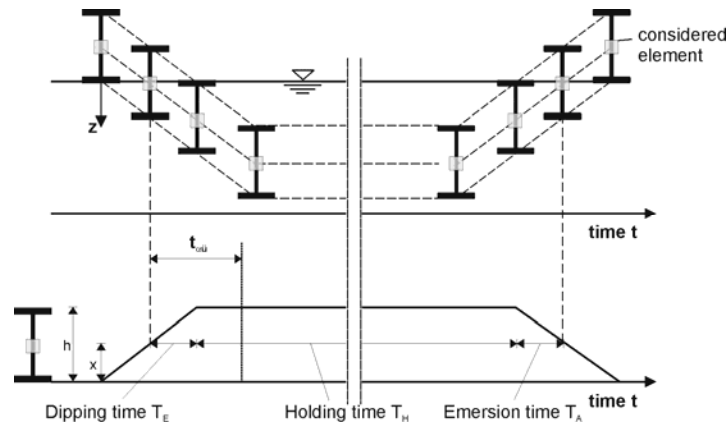


Fig. 9-5: Time history of dipping for a mass particle of the structural component

- (1) Fig. 9-5 shows the dipping procedure versus time and fig. 9-6 gives an example of the temperature distributions over a selected cross-section resulting in residual strain distributions that are laid over the residual strain distributions of the steel component from fabrication.
- (2) The residual strains that arise from the temperature distribution are shown in fig. 9-7.

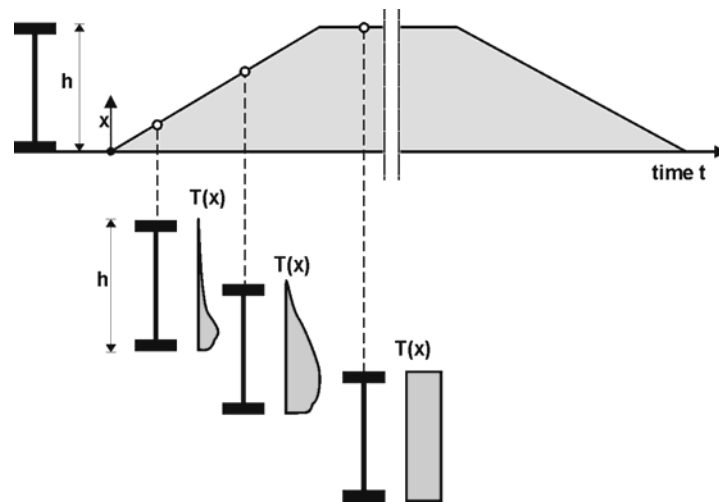


Fig. 9-6: Time history of temperature for a cross-section of a structural component

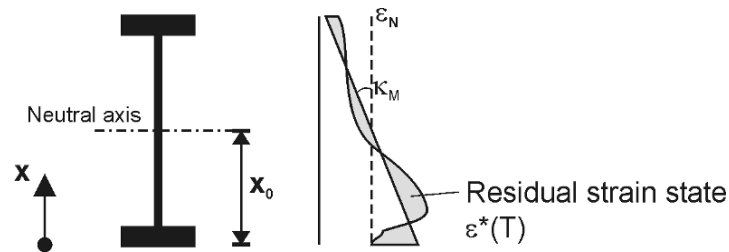


Fig. 9-7: Residual strain increments from temperature distributions

9.4 Superposition of stationary and instationary strains

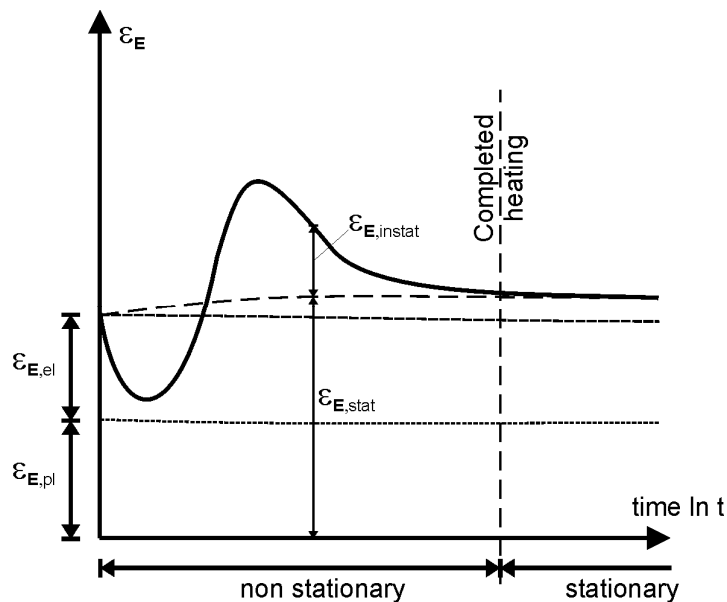


Fig. 9-8: Example of a time history of equivalent plastic strain requirements

- (1) Fig. 9-8 gives the principle of the time history of equivalent plastic strain from fabrication ($t=0$), superimposed with strains from the heating with the time variant temperature distributions until full heating is achieved (situation without any temperature gradient). The full equivalent plastic strain accumulation process including stress relief by the exposure to the zinc bath is relevant for the strain requirement at a certain time.

9.5 Conclusions from variation of detail and plate thickness

- (1) FEM-calculations of the instationary component of the strain history have been performed with variation of:
- the structural detail considered, see fig. 9-9,
 - the immersion speed during dipping into the smelter, see fig. 9-10,
 - the alloy with varying heat transition coefficients, see fig. 9-11.

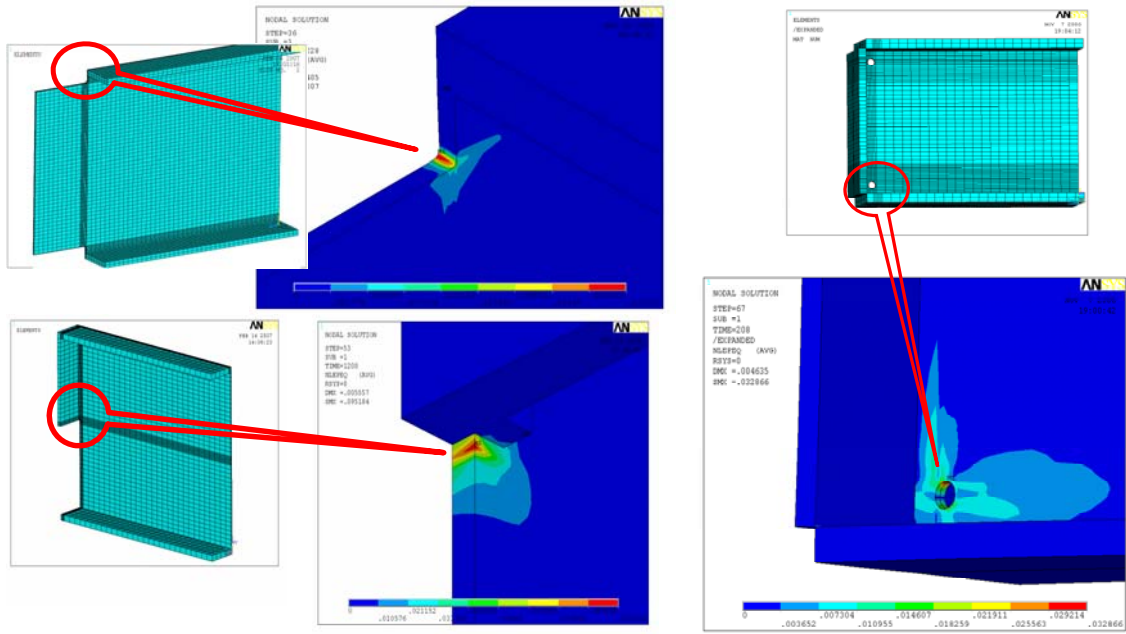


Fig. 9-9: Calculation of maximum strains for different details

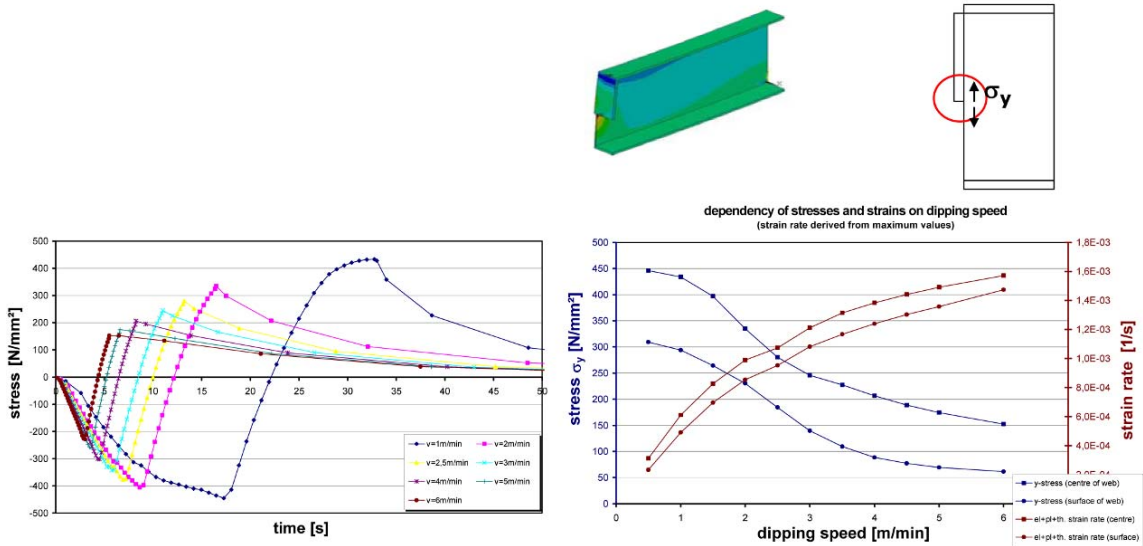


Fig. 9-10: Stress-time histories for different dipping speeds

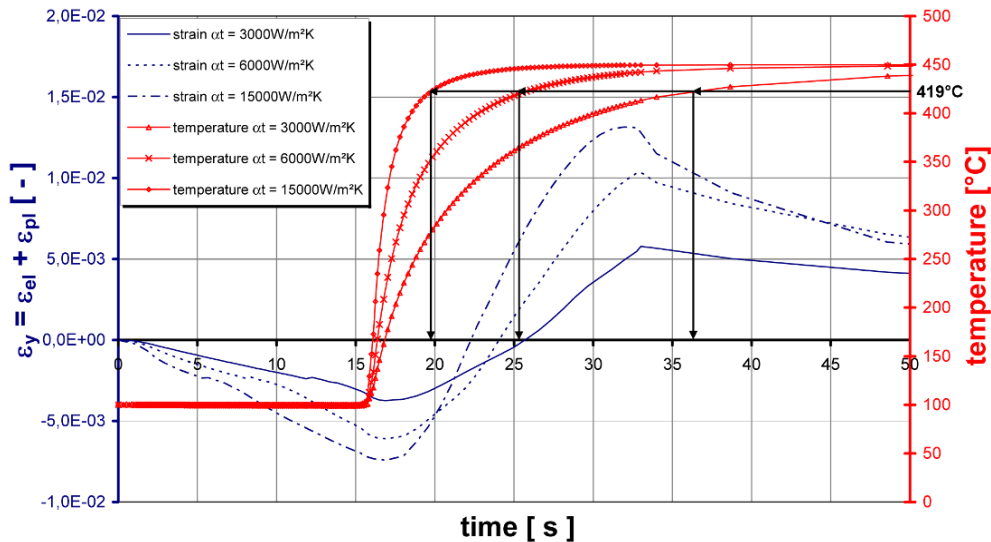


Fig. 9-11: Effect of different zinc-alloys with different heat-transition coefficients at on temperature- and equivalent strain-histories

- (2) Fig. 9-12 gives examples for the instationary part of the equivalent plastic strain requirements ε_E for two alloys and immersion speeds representing the normal conditions before and after actions were undertaken to reduce damages [75]:

Before actions: zinc alloy class 3 with the parameters:

$$\begin{aligned} v &= 0,25 \text{ m/min (immersion speed)} \\ \alpha_t &= 15.000 \text{ W/m}^2\text{K (heat transfer coefficient)} \\ T_V &= 50^\circ\text{C (preheating temperature)} \\ T_{Bath} &= 450^\circ\text{C} \end{aligned}$$

After actions: zinc alloy class 1 with the parameters:

$$\begin{aligned} v &= 0,80 \text{ m/min} \\ \alpha_t &= 3.000 \text{ W/m}^2\text{K} \\ T_V &= 20^\circ\text{C} \\ T_{Bath} &= 450^\circ\text{C} \end{aligned}$$

The data apply for various details and steel grade S355J2. They show for the details that are comparable, that zinc alloy 1 in connection with higher dipping speeds gives smaller strain requirements.

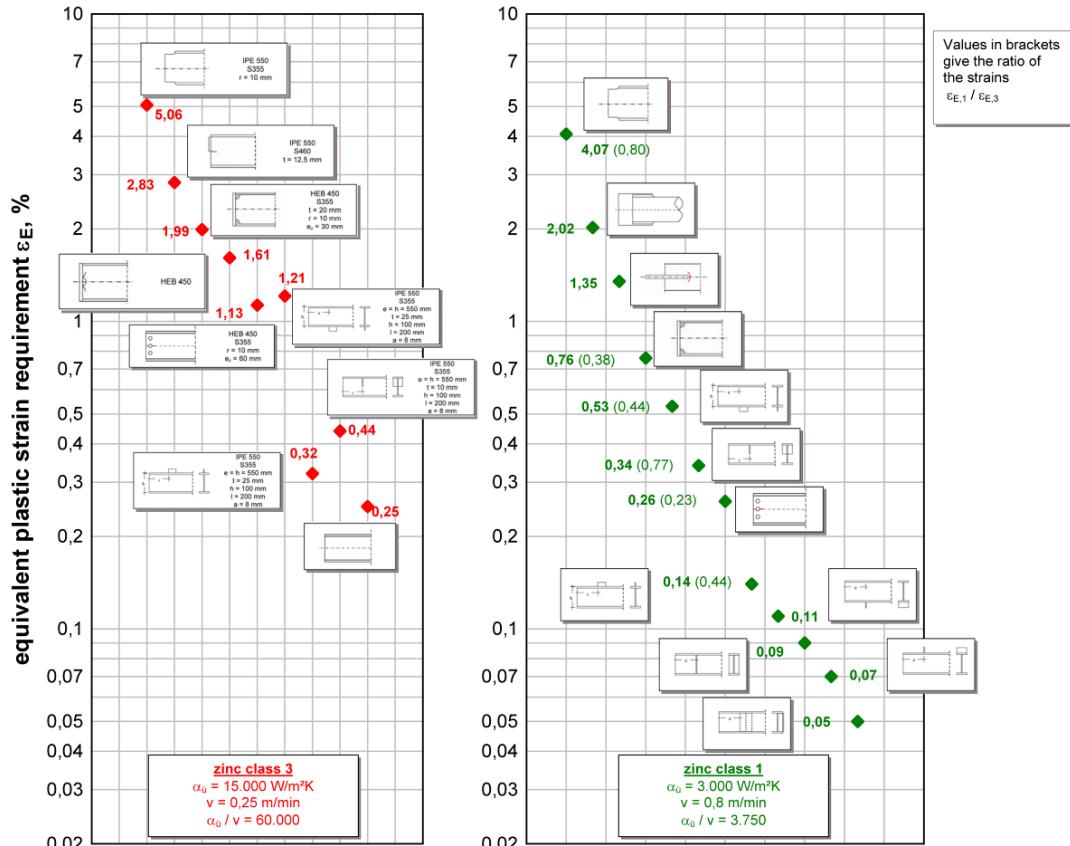


Fig. 9-12: Examples of equivalent plastic strain requirements in zinc alloy classes 3 and 1 and different dipping speeds and preheating temperatures for various details, see also [fig. 10-2](#)

- (3) [Fig. 9-13](#) gives the stationary part of the equivalent plastic strain ϵ_E resulting mainly from the fabrication of the prefabricated steel component and its constitutive material, e.g. by rolling, cold forming and welding and the relieving effect of the liquid zinc bath. These values are correlated with the thickness s of steel and the process time of the steel material in the liquid zinc bath.

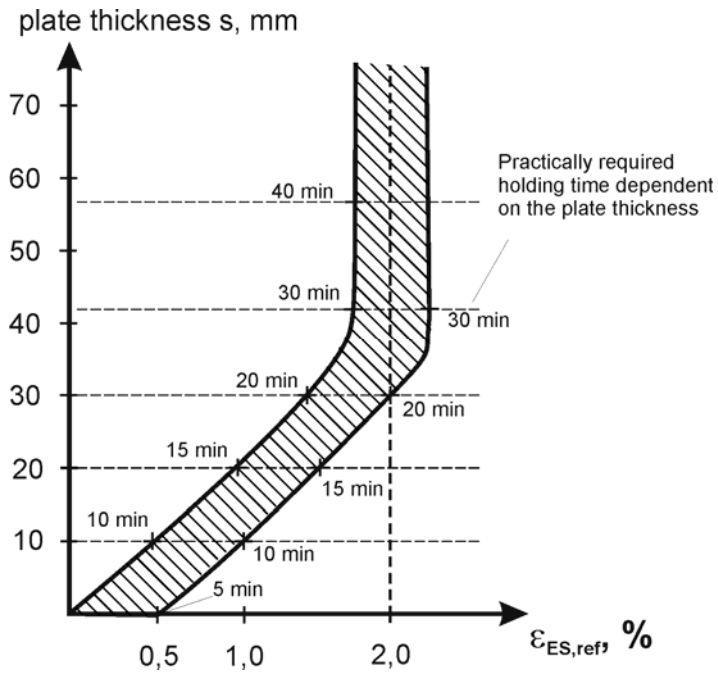


Fig. 9-13: Relationship between ϵ_{ES} , s and dipping time t_s

10 Limit state assessments based on equivalent plastic strains

- (1) The mechanical background of the two design situations used for the limit state assessments to avoid cracking in the zinc bath is given in [fig. 10-1](#).

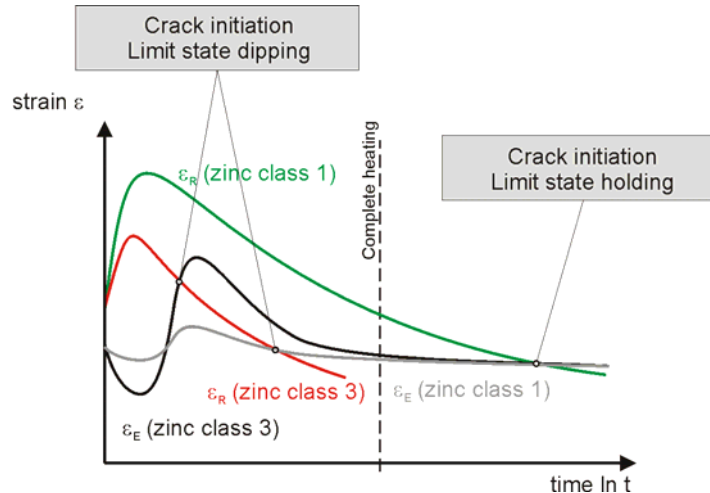


Fig. 10-1: Cases a) and b) for the limit state assessment

- (2) This figure demonstrates the principle of the limit state assessment for two zinc alloys with different aggressiveness:

case a: For a highly aggressive zinc alloy (e.g. zinc class 3) the peak value of the time history of strain-requirements reached during the dipping process is relevant for cracking. Cracks may occur during the submerging of the structural component into the zinc bath and appropriate measures to reduce the risk are related to reducing the peak value by preheating or reducing the time required for full submergence.

case b: For moderate and low aggressive zinc alloys (e.g. zinc class 1), the exposure time in the zinc bath leading to a reduction of strain resistance is relevant for cracking, and appropriate measures to reduce the risk are related to reducing the exposure time by reducing the thickness of plates and the differences in thickness of plates.

- (3) For case a) design situation during the dipping phase-, [fig. 10-2](#) gives the results of the ratios η

$$\eta = \frac{\varepsilon_E}{\varepsilon_R} \quad (10.1)$$

for the typical conditions before and after actions to reduce damages [75]

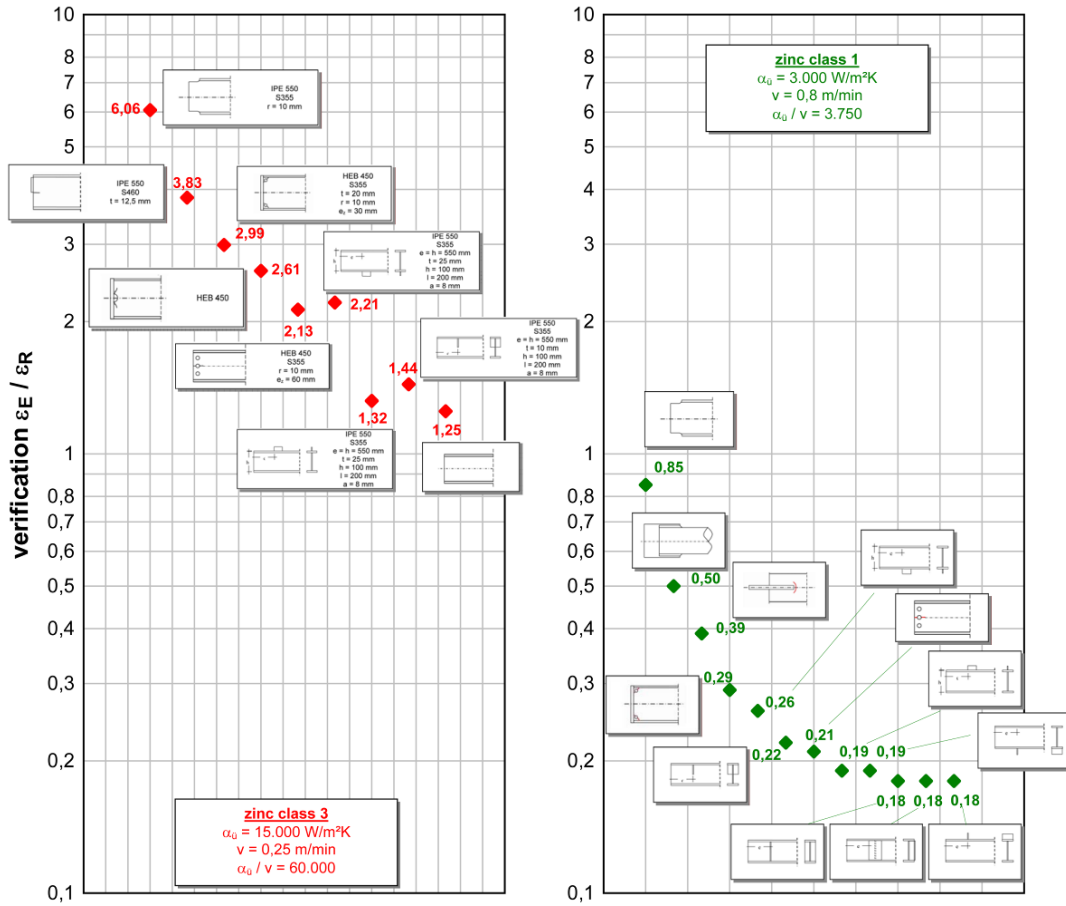


Fig. 10-2: Comparison of equivalent plastic strain requirements ϵ_E and plastic strain resistance ϵ_R in zinc alloy classes 3 and 1 and different dipping speeds and preheating temperatures for various details, see also fig. 9-12

Apparently the content of tin has a dominant effect and zinc alloy class 3 should not be used for many details that are frequently applied in practice, whereas zinc alloy class 1 is applicable for all details investigated.

- (4) Fig. 10-3 gives a further detail for the determination of η for beams with end plates and cut outs, which identifies the effect of the depth of beams as observed by damages.

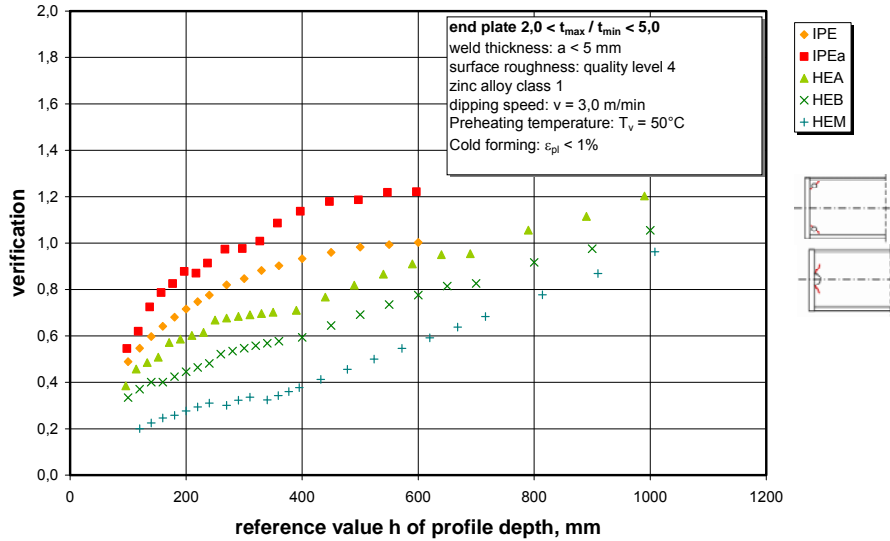


Fig. 10-3: Ratios η for different beam depths, based on equation (12.8)

- (5) For case b) -design situation during the holding phase- [fig. 10-4](#) gives the conclusions for the holding time t_S from

$$t_S = \frac{5\varepsilon_{R,ref}^*}{\varepsilon_R(t_S)} [\text{min}] \tag{10.2}$$

using the assumptions given in [fig. 8-6](#).

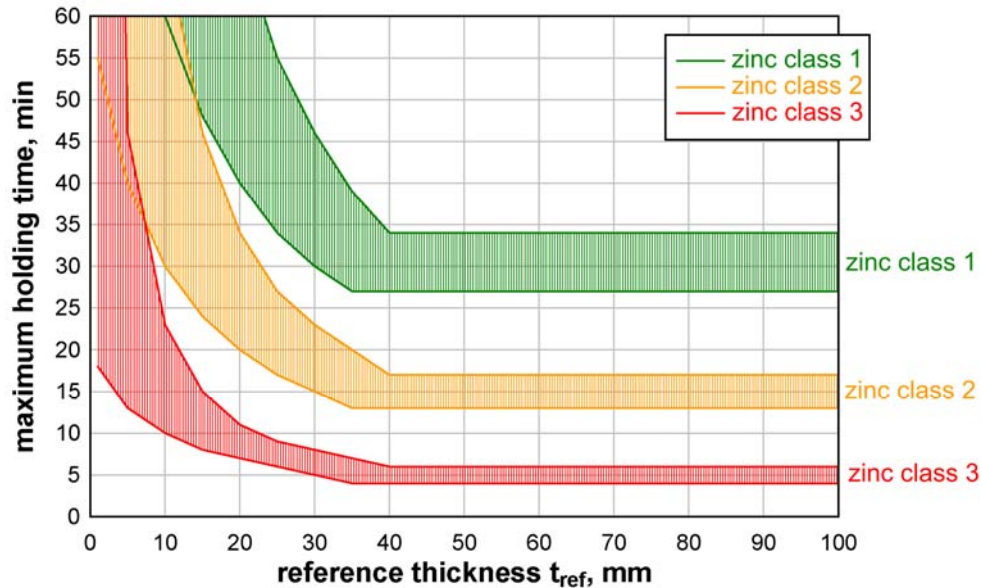


Fig. 10-4: Relationship between the plate thickness s resp. the reference thickness t_{ref} and the maximum holding time in the zinc bath for zinc alloy class 1, 2 and 3

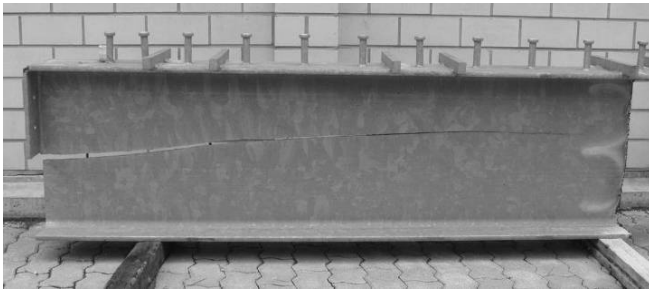
Based upon this research, common steel component thickness can be hot dip galvanized in a zinc melt class 1 with no risk of cracking.

11 Validation of the strain-oriented assessment method

11.1 General

- (1) In the following examples for cracks observed after galvanizing or after erection of hot-dip galvanized components are given, which look plausible if compared with the assessment method based on equation (10.1) and (10.2).
- (2) Apparently the type of zinc alloy is a main parameter; zinc alloys according to zinc class 1 would reduce the problems to mainly structural aspects as choice of steel, cross-section and structural detailing in connection with procedural aspects as dipping speed and holding time.
- (3) The following examples also give an impression how cracks starting at typical crack initiation points look like.

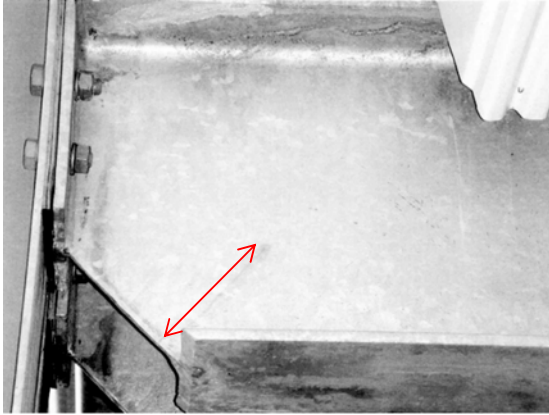
11.2 Structural components from car-parkings



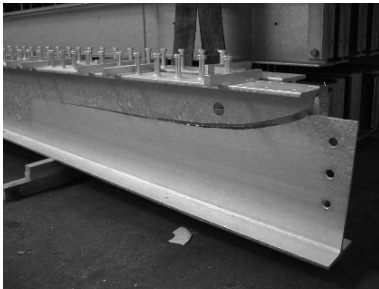
Construction: IPE550, $l \sim 16$ m
 Detail: half endplate $t = 12,5$ mm
 Material: S460N, large KV-value in web
 Zinc alloy: 0,8 Pb + 1,1 Sn + 0,07 Bi
 Crack: starting from end of endplate, $l = 1800$ mm



Construction: IPE450, $l \sim 16$ m, $t_{\text{Endplate}} = 12,5$ mm
 Detail: half endplate with cut out $d = 30$ mm
 Material: S460N
 Zinc alloy: 1,0 Pb + 1,1 Sn + 0,08 Bi
 (alloy composition does not comply with EN ISO 1461)
 Crack: starting from cut out, $l = 200$ mm

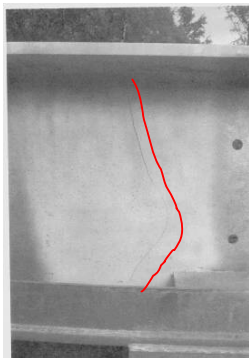


Construction: I \approx 16 m
Detail: half endplate with oblique cut
Material: -
Zinc alloy: -
Crack: starting at end of radius in web at bottom flange; l \sim 250 mm



Construction: IPE 550, l \sim 16 m
Detail: cope cut with radius d = 12 mm
Material: S460
Zinc alloy: 0,2 Pb + 0,6 Sn + 0,1 Bi
Crack: starting at end of radius at cut out; l \approx 1500 mm

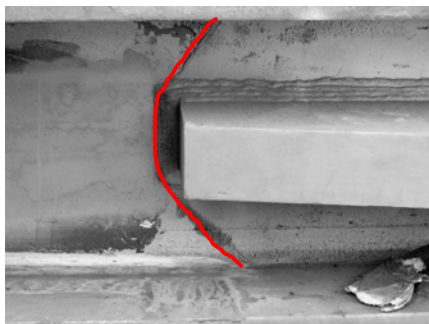
11.3 Further prefabricated beams



Construction: HEA 550, l = 18 m
Detail: as rolled
Material: copper 0,3%
Zinc alloy: 1,0 Pb + 0,6 Sn + 0,02 Bi
Crack: across full depth of web, l \approx 550 mm
and across part of flange, l \approx 100 mm



Construction: HEB 1000, $l = 18$ m
 Detail: holes, $d = 36$ mm
 Material: -
 Zinc alloy: $0,9 \text{ Pb} + 0,8 \text{ Sn} + 0,02 \text{ Bi}$
 Crack: starting at holes, $l \approx 250$ mm



Construction: HD 400 x 509, main tension chord of a lattice girder in a stadium roof
 Detail: plate inserted in web, $t_{pl} = 80$ mm
 Material: S355 J2 G3
 Zinc alloy: $1,0 \text{ Pb} + 1,1 \text{ Sn} + 0,04 \text{ Bi}$
 (alloy composition does not comply with EN ISO 1461)
 Crack: crescent-like crack at the end of inserted plate through entire web and parts of top and bottom flange, $l \sim 400$ mm

11.4 Prefabricated columns

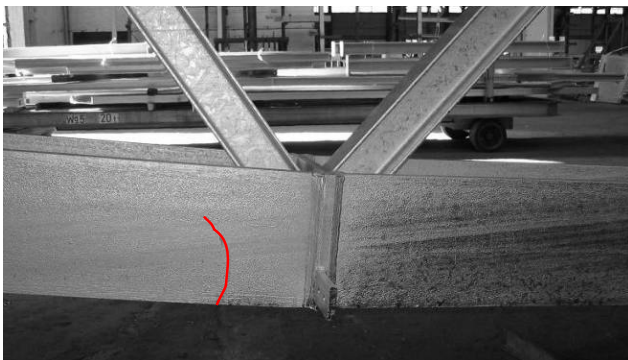


Construction: HEB 340
 Detail: horizontal and vertical attachments, $t_{pl} = 30$ mm and $t_{pl} = 50$ mm with holes and cut outs
 Material: S355 J2 G3
 Zinc alloy: $0,3 \text{ Pb} + 0,9 \text{ Sn} + 0,08 \text{ Bi}$
 Crack: starting at holes and cut outs, $l \sim 50$ mm; at welds $l \sim 30$ mm

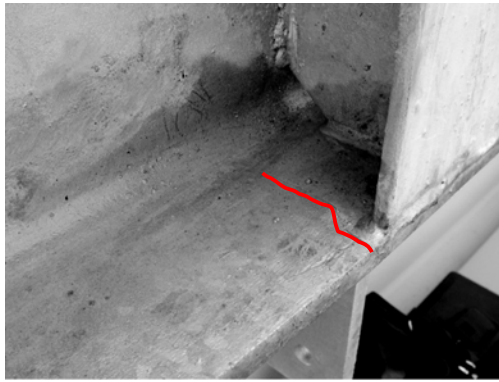


Construction: HEM 300
Detail: footplate connection with cut outs $r = 50$ mm, $a_{\text{weld}} = 18$ mm
Material: S355 J2 G3
Zinc alloy: 0,9 Pb + 0,8 Sn + 0,02 Bi
Crack: starting at cut out: running into the web, $l \sim 100$ mm; running along weld toe, $l \sim 100$ mm

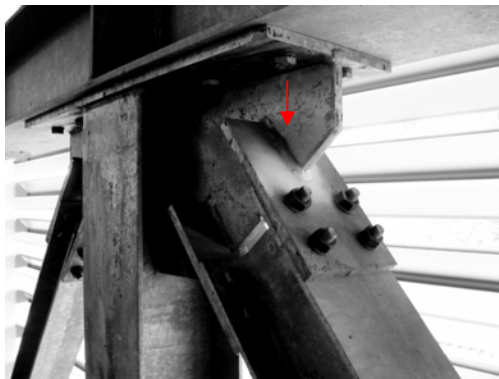
11.5 Latticed structures



Construction: HEA 400 in a chord of a lattice girder, with an additional longitudinal plate between flanges to form a boxed section
Detail: box type element with small drainage holes
Material: S355 J2 G3; microstructure and KV-value at lower bound limits
Zinc alloy: 1,0 Pb + 0,8 Sn + 0,14 Bi
Crack: starting at edge of flange of rolled section running towards midline, $l \sim 250$ mm



Construction: HEA 400
Detail: transverse stiffener
Material: S355 J2 G3; microstructure and KV-value at lower bound limits
Zinc alloy: 1,0 Pb + 0,8 Sn + 0,14 Bi
Crack: starting at flange edge, l ~ 150 mm



Construction: welded built-up connection element
Detail: lamellas inserted into gusset plate
Material: S355 J2 G3
Zinc alloy: 1,0 Pb + 0,9 Sn + 0,02 Bi
Crack: starting at weld-around, l ~ 60 mm

11.6 Cold-formed components



Construction: IPE 450, l ≈ 16 m; Precambered by cold forming
Detail: local imprint in flange surface from tool for 3-point plastic bending
Material: S460 N
Zinc alloy: 1,0 Pb + 1,1 Sn + 0,08 Bi
Crack: transverse to the flange, l ≈ 200 mm

11.7 Hollow section components



Construction: welded box girder, $t = 8 \text{ mm}$; $a_{\text{weld}} = 5 \text{ mm}$
Detail: longitudinal fillet welds
Material: S355 J2 G3
Zinc alloy: 0,7 Pb + 0,2 Sn
Crack: starting at edge, $l \sim 70 \text{ mm}$



Construction: circular hollow section, RO273 x 6,3, acting as tension rod for a stadium roof (suspension)
Detail: inserted gusset plate
Material: S355
Zinc alloy: 0,9 Pb + 0,8 Sn + 0,01 Bi
Crack: starting at end of gusset plate, $l \approx 20\text{-}100 \text{ mm}$

12 Transfer of results based on equivalent plastic strains into engineering models for practical assessments

- (1) The limit state assessment based on equivalent plastic strain may be used as background procedure for developing more easy-to-use rules for practical application.
- (2) Such easy-to-use rules may be based on assessment formulae applicable both for case a) – the dipping process – and case b) – the holding phase –, see [fig. 12-1](#). The formulae are derived in [section 13](#), where it is shown, that the results are equivalent to the results of an assessment with equivalent plastic strains.

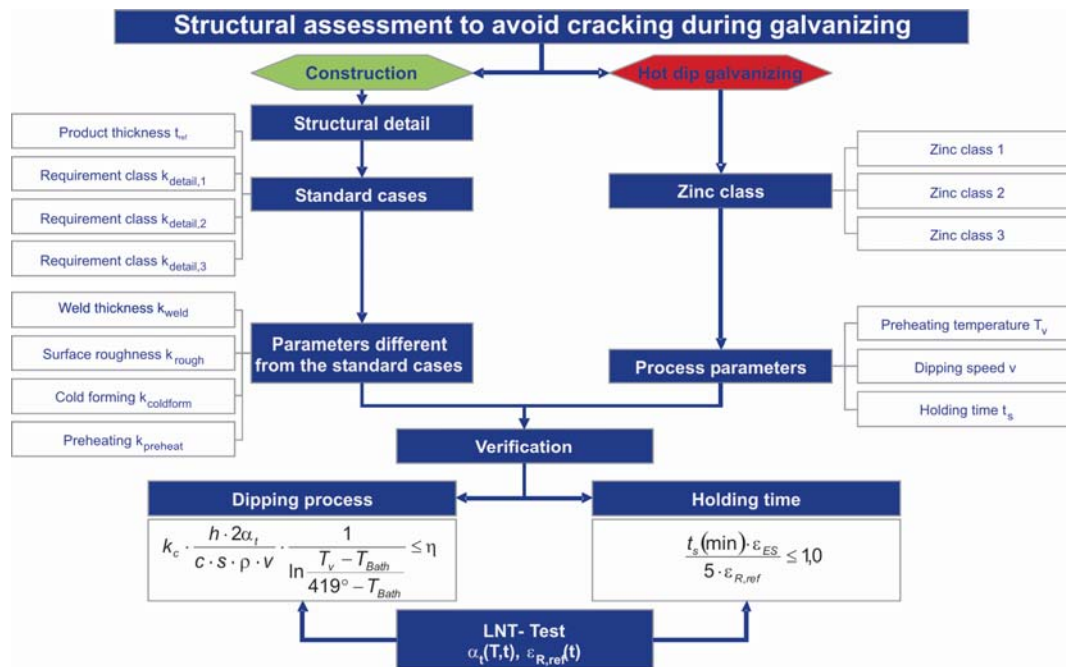


Fig. 12-1: Flow chart for the structural assessment to avoid cracking from liquid metal embrittlement

- (3) A further step of simplification is an assessment procedure based on technical classes, that avoids any numerical verification. This procedure is given in [section 15](#).
- (4) Both the simplified assessment method in [section 13](#) and the classification method in [section 15](#) apply to certain conditions for:
 - design of the prefabricated structural steel components,
 - the semifinished (constituent) products,
 - the structural detailing and fabrication of steel components,
 - the preparation of steel components prior to the hot-dip-zinc-coating,
 - requirements for the zinc bath,
 - testing of the zinc bath,

which are addressed in [section 14](#) of this report.

- (5) All the practical assessment procedures are calibrated to laboratory tests, numerical simulations and experiences. They use technical classes so that deliveries with crack sizes that may infringe the structural safety are excluded. Due to the large scatter of results a quantification of the reliability index for achieving freedom of relevant cracks is however not yet possible. Therefore confidence zones as specified in section 14 are introduced.

13 Simplified engineering models for numerical assessment

- (1) In order to obtain a simple engineering model for assessing the dipping process, a rectangular plate with the plate thickness s and the depth h is assumed to be dipped with the velocity v into the liquid zinc bath. The plate is supposed to be without residual stresses or strains, see [fig. 13-1](#).

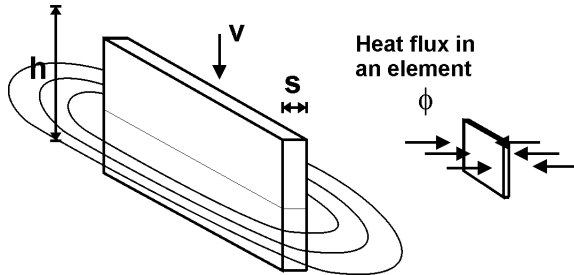


Fig. 13-1: Reference model for the dipping process

- (2) This reference model is used for the following purposes:
1. to calculate the time $t_{\alpha t}$ of a particular plate-element, see [fig. 13-1](#), to heat up from the preheating temperature T_V to the melting temperature of pure zinc $T_a = 419^\circ\text{C}$,

In this calculation, the heat conductivity through the plate thickness is neglected. The heat transfer coefficient α_t is taken as the actual effective value for the zinc alloy in question,
 2. to determine the time history of instationary residual stresses and strains caused by strains ε^* from temperature differences from dipping with different velocities v to identify the time t_σ when the maximum of residual stresses and strains occurs,
 3. to use the pseudo-limit state criterion based on the assumption that in the beginning of the heating up phase the zinc coat freezes at the “cold” surface of the steel component and hence reduces the corrosion effect of the zinc alloy until the steel component has adopted the temperature of the zinc bath (cracking of the frozen zinc layer is not considered).

Based on this assumption, the limit state is defined by the requirement, that the time interval t_σ for attaining the maximum of the time history of residual stresses should be smaller than the heating up time $t_{\alpha t}$:

$$t_\sigma - t_{\alpha t} \leq 0 \quad (13.1)$$

or

$$\frac{t_\sigma}{t_{\alpha t}} \leq 1 \quad (13.2)$$

4. to link the simplified limit state equation (13.2) to the actual limit state for equivalent plastic strains as given in fig. 10-1 case a) by adaption factors k_c , see (8).
- (3) The calculation of the reference time t_{α} in fig. 13-1 is based on the following assumptions:

1. The heat transfer between the zinc bath and the steel plate is constant with time:

$$C\rho V \frac{dT}{dt} = \alpha_t A (T_a - T) \quad (13.3)$$

where

- C is the specific heat capacity of the plate
 ρ is the specific mass
 V is the volume of the plate
 T is the temperature of the plate
 t is the time
 α_t is the effective heat transfer coefficient for the zinc alloy
 A is the surface of the plate
 T_a is the melting temperature of pure zinc (419°C)
 T_{Bath} is the temperature of the zinc bath.

2. The first zinc coat freezes on the plate surface and prohibits further access of aggressive constituents of the zinc alloy to the steel surface, thus protecting the steel from cracking. Any cracking of the frozen zinc coat is not considered.

- (4) Equation (13.3) leads to:

$$dt = \frac{CV\rho}{A\alpha_t} \frac{dT}{T_a - T} \quad (13.4)$$

which gives

$$t_{\alpha} = \frac{C \cdot s \cdot \rho}{2 \alpha_t} \int_{T_V}^{T_a} \frac{dT}{T_a - T} = \frac{C \cdot s \cdot \rho}{2 \cdot \alpha_t} \ln \frac{T_V - T_{Bath}}{419^\circ C - T_{Bath}} \quad (13.5)$$

- (5) For the example of a plate with

- s = 0,01 m
 T_{Bath} = 450°C
 T_V = 50°C
 α_t = 6000 W/m²K
 C = 600 J/kg · K
 ρ = 7.800 kg/m³

the temperature-time curve is given in fig. 13-2.

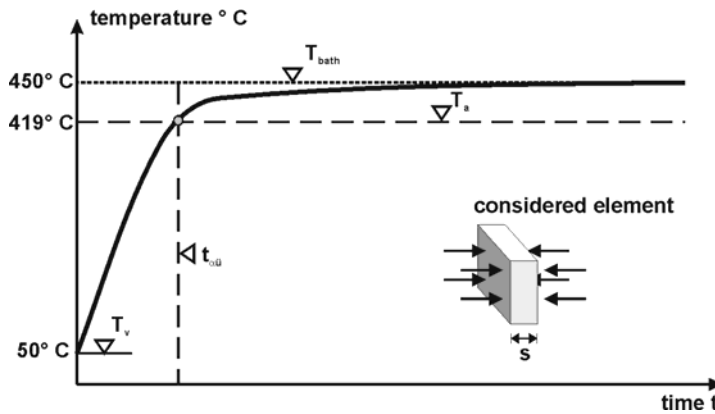


Fig. 13-2: Examples for a temperature-time curve

- (6) The pseudo-limit state equation for the reference model in fig. 13-1 reads:

$$\frac{h}{v} - \frac{Cs\rho}{2\alpha_t} \ln \frac{T_v - T_{Bath}}{419^\circ\text{C} - T_{Bath}} \leq 0 \quad (13.6)$$

or:

$$\frac{2\alpha_t h}{Cs\rho v} \cdot \frac{1}{\ln \frac{T_v - T_{Bath}}{419^\circ\text{C} - T_{Bath}}} \leq 1 \quad (13.7)$$

- (7) For the example of a plate with $h = 0,50$ m, $s = 0,01$ m without residual stresses and strains, the time histories of stresses during the submerging process are given in fig. 13-3 for various dipping velocities.

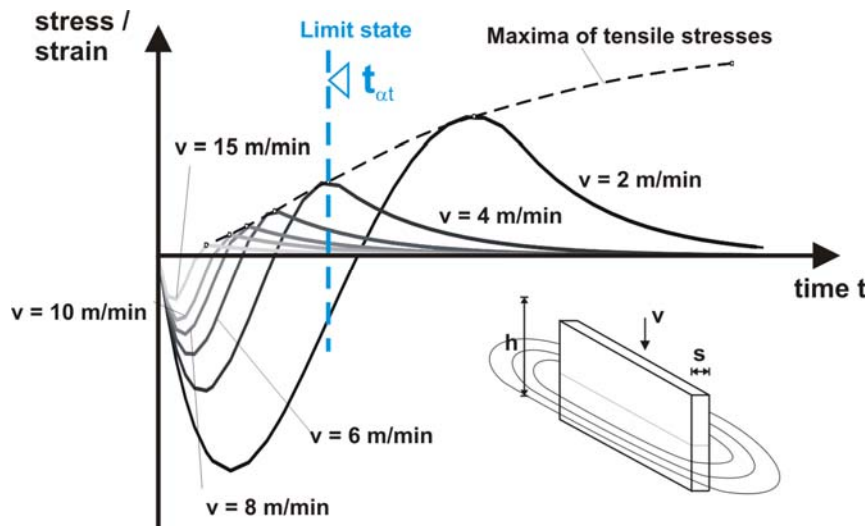


Fig. 13-3: Time histories of residual stresses for various dipping velocities where the pseudo-limit state is reached for $v = 3,5$ m/min

In this figure the pseudo-limit state is reached for a velocity $v = 3,5/\text{min}$.

- (8) The link of the limit state of this model to the limit state of the model based on strain assessment is given in fig. 13-4, where on the left side the limit state condition $\frac{t_\sigma}{t_{at}} \leq 1$ is given for the engineering model and on the right side the role of the adaption factor k_c is shown to adjust the value t_{at} of the engineering model to the value

$$t_{at}^* = \frac{t_{at}}{k_c} \tag{13.8}$$

consistent with the assessment model for strains.

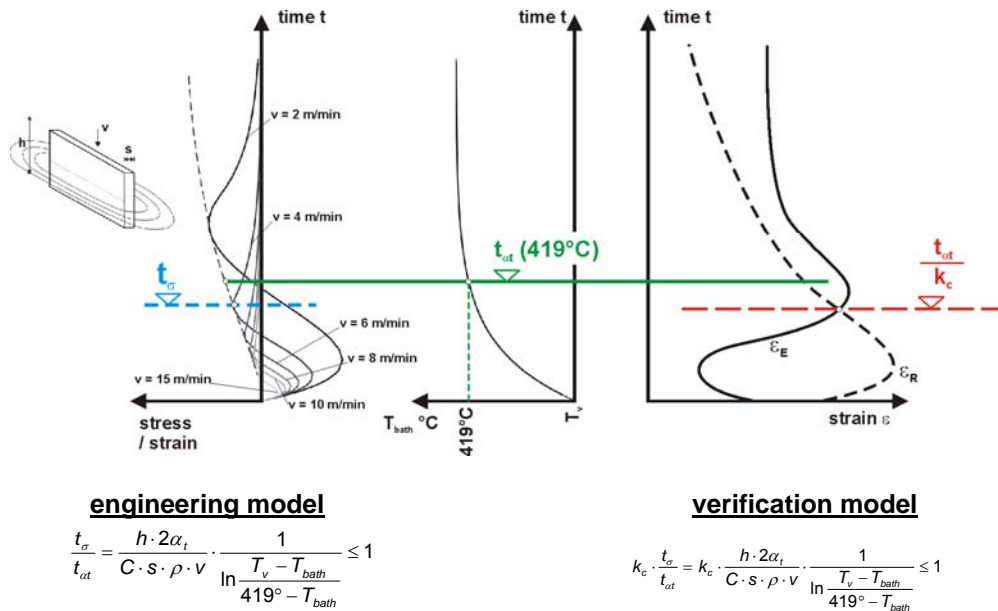


Fig. 13-4: Conditions for the attainment of the pseudo-limit state

- (9) In conclusion, the basic formula for verifying freedom of cracks from hot-dip-galvanizing is

$$k_c \cdot \frac{h \cdot 2\alpha_t}{C \cdot s \cdot \rho \cdot v} \cdot \frac{1}{\ln \frac{T_v - T_{Bath}}{419^\circ\text{C} - T_{Bath}}} \leq \eta \tag{13.9}$$

where η is the utilisation rate, that theoretically should not exceed the value $\eta = 1,0$, see figure 13-4.

- (10) Fig. 13-5 gives more details to determine the adaption value k_c from equation (13.8):

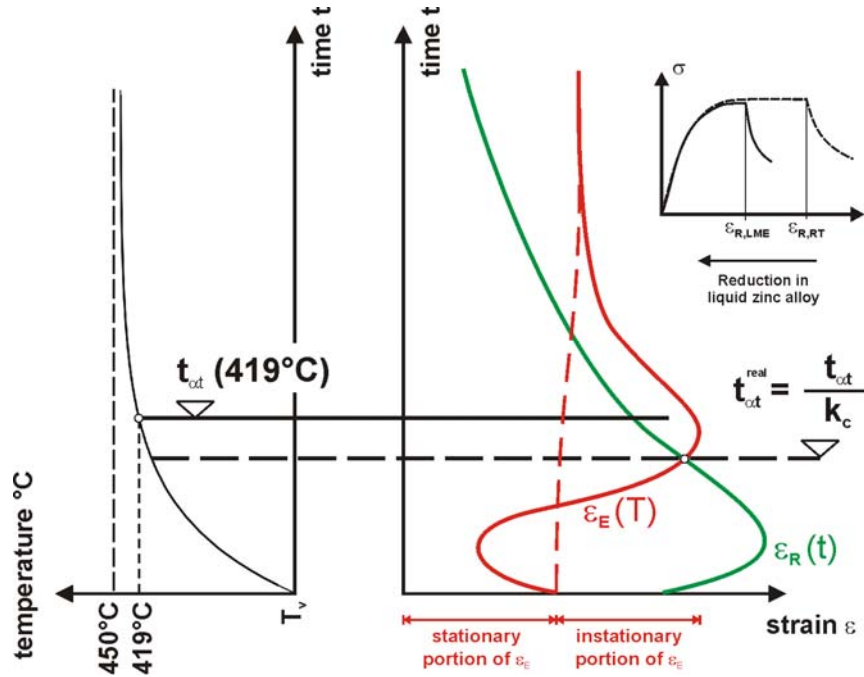


Fig. 13-5: Determination of t_{ct}^{real} and t_{ct} to determine k_c

- (10) The factor k_c is composed of the following components:

$$k_c = k_{detail} \cdot k_{weld} \cdot k_{surface} \cdot k_{coldform} \cdot k_{preheat} \quad (13.10)$$

where

k_{detail}	represents the structural detailing
k_{weld}	represents the weld thickness
$k_{surface}$	represents the surface roughness
$k_{coldform}$	represents the effects of prestraining by cold forming
$k_{preheat}$	represents the effects of T_V in addition to its effect in the limit state formula.

- (11) The adjustment factor k_c takes the value 1,0 for the following conditions:

- strain requirement	$\leq 2,0 \%$
- weld thickness	$a < 7 \text{ mm}$
- roughness of cut surfaces and surfaces according to EN ISO 9013	quality level 4
- grade of cold forming	$\varepsilon_{pl} < 1\%$
- preheating temperature	$T_V \leq 50^\circ\text{C}$

- (12) Where these conditions are not met the value of k_{detail} may be taken from [fig. 13-6](#) and those of the other k -values from [fig. 13-7](#).

Detail class	ε_E	Detail	k_{detail}
A	$\leq 2\%$	Profiles without attachment parts, constant section, no constructive notches All rolled sections: I, IPE, HEA, HEB, HEM Welded sections taking into account the thickness ratio $t_{max}/t_{min} \leq 1,5$ Profiles with attachment parts, constant section, constructive notches in terms of attachments taking into account the thickness ratio $t_{max}/t_{min} \leq 1,5$ Distance e of attachment to end of beam: $e > h$ Holes $d \geq 25 \text{ mm}$	0,3
B	$\leq 6\%$	Profiles with attachment parts, constant section, constructive notches in terms of attachments taking into account the thickness ratio $1,5 < t_{max}/t_{min} < 5$ Holes $d < 25 \text{ mm}$ nodes of lattice girders hollow sections with connection plates	0,5
C	$\leq 12\%$	Profiles with constructive notches at the free end of a beam	0,8

Fig. 13-6: Classification of structural details and k_{detail} -values

Adjustment coefficient		k
Weld thickness	$a \leq 5 \text{ mm}$	1,00
	$5 \text{ mm} < a \leq 12 \text{ mm}$	1,25
	$12 \text{ mm} < a$	1,50
Surface roughness according to EN ISO 9013, table 5	Quality level 4	1,00
	Quality level 1-3	1,20
Cold forming	$\varepsilon_{pl} \leq 1\%$	1,00
	$1\% < \varepsilon_{pl} \leq 5\%$	1,10
	$5\% < \varepsilon_{pl} < 20\%$	1,25
Preheating temperature-effects on yield strength	$T_V \leq 50 \text{ }^\circ\text{C}$	1,00
	$50 \text{ }^\circ\text{C} < T_V < 200 \text{ }^\circ\text{C}$	$1,10 - T_V / 400$

Fig. 13-7: Classification of weld, surface, cold forming- and preheating effects

(13) For a standard process of zinc-coating that could be defined e.g. with the following parameters:

- zinc alloy class 1
- $\alpha_{t,eff} = 3000 \text{ W/m}^2 \text{ K}$
- dipping speed $v = 0,8 \text{ m/min}$
- preheating temperature $T_V = 20^\circ\text{C}$

the assessment formula (13.9) could be simplified to

$$k_c \cdot \frac{h}{s} \frac{1}{27} \leq \eta \quad (13.11)$$

- (14) For the verification of the holding time via formula (10.2) and for the zinc alloy class 1 see (13) the permissible holding time dependant on the plate thickness may be taken from [fig. 13-8](#).

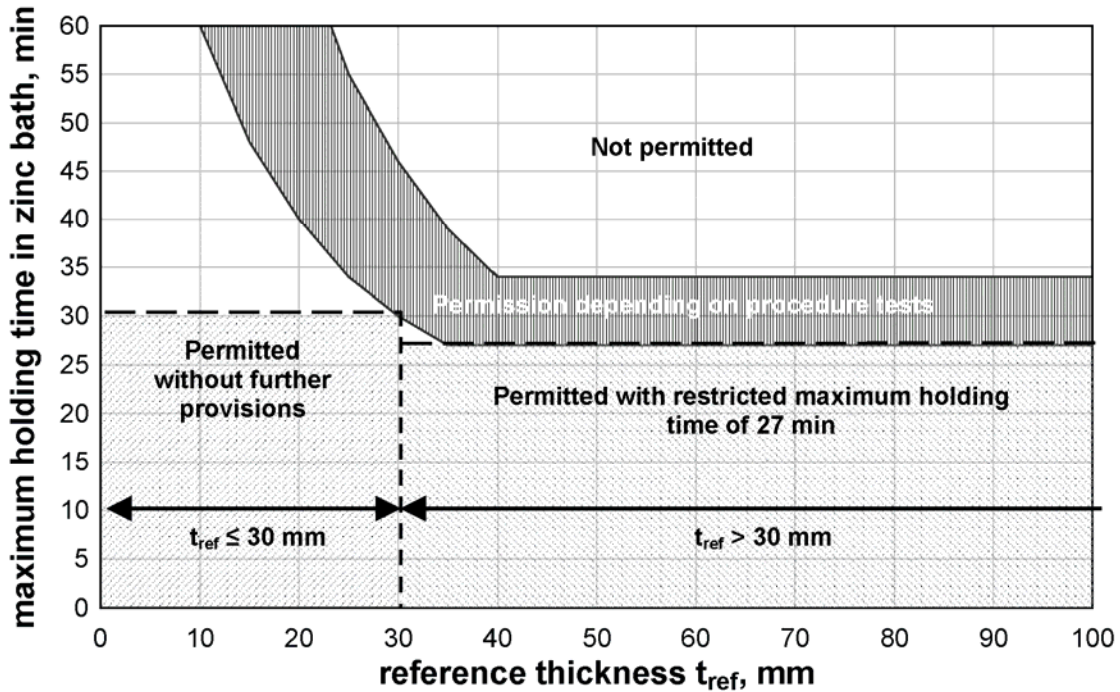


Fig. 13-8: Maximum holding time in the zinc bath for zinc alloy class 1 (see (13))

- (15) For plate thickness $t_{ref} \leq 30 \text{ mm}$ the usual holding time is smaller than 30 min, so that no extra provisions apply. For $t_{ref} > 30 \text{ mm}$ the limitation of the holding time to 27 min (without further procedure tests) should be observed.

14 Introduction of Confidence zones

(1) The limit state conditions in equation (10.2) and (13.9) are based on assumptions for the classification of thicknesses and details as well as for constituent products and for fabrications as follows:

1. Constituent steel products are free of “crack like defects” on the surface according to EN 10163-Part 2 for plates and EN 10163-Part 3, Class C subgroup 1 for long products.

In particular long products with large depths are produced such that residual stresses and differences of yield strength and impact energy across the cross-section are kept small.

The chemical composition of steels in particular those produced on the scrap-route should be controlled, and meet the requirements for good weldability.

2. Residual strains caused by fabrication are limited by appropriate detailing, weld preparation, welding procedures and welding sequences e.g.:

- welding of butt welds before fillet welds,
- no intermitted welds,
- flexible assembly,
- accurate and sufficiently robust tackling,
- no exceedance of weld thicknesses required by design.

3. At welds a component has preferably almost equal plate thicknesses; where the ratio of plate thicknesses exceeds $\frac{\max t}{\min t} = 5$, the component should be separated by assembly joints.

4. The superposition of residual strains from thermal cutting at edges and from welding is avoided by a minimum excess length for fillet welds of $2a + 3$ mm where a is the weld thickness. The same value applies for the minimum distance of edges of holes to welds.

5. Critical micro-cracks from thermal cutting and punching are avoided by:

- considering either a maximum surface hardness of 340 HV according to EN ISO 14713 and fabrication of punched holes with undersize and reaming to normal size as for structures subjected to fatigue loads,
- or fabrication of punched holes or cold-cut edges according to requirements of procedure tests.

6. Excessive cold-forming effects are excluded by:

- considering either the strain limits $\varepsilon_{plast} = \frac{t}{2r+t} \leq 2\%$

where

t is the plate thickness,
 r is the inner radius of cold forming
 or annealing in cold formed areas,

- application of appropriate “notch-free” tools for cold forming,
- no punch marking except at locations where cracking is not expected to occur (e.g. at end plates).

(2) In order to take account of the large scatter of strain requirements and strain capacities and of the model uncertainty in particular in equation (13.9) the notion of Confidence Zones has been introduced, that gives a relation between the utilisation rate η in equation (13.9) and the necessary provisions for inspections, see figure 14-1.

Steel grade	Detail Class		
	A	B	C
S235	$\eta \leq 0,7$ Confidence Zone 1 $0,7 < \eta \leq 1,2$ Confidence Zone 2 $\eta > 1,2$ Confidence Zone 3	$\eta \leq 1,2$ Confidence Zone 1 $\eta > 1,2$ Confidence Zone 2	$\eta \leq 1,2$ Confidence Zone 1 $\eta > 1,2$ Confidence Zone 2
S275		$\eta \leq 0,7$ Confidence Zone 1 $0,7 < \eta \leq 1,2$ Confidence Zone 2 $\eta > 1,2$ Confidence Zone 3	$\eta \leq 1,0$ Confidence Zone 1 $1 < \eta \leq 1,2$ Confidence Zone 1 $\eta > 1,2$ Confidence Zone 3
S355			$\eta \leq 1,0$ Confidence Zone 1 $1 < \eta \leq 1,2$ Confidence Zone 2 $\eta > 1,2$ Confidence Zone 3
S460			$\eta \leq 1,0$ Confidence Zone 2 $1 < \eta \leq 1,2$ Confidence Zone 2 $\eta > 1,2$ Confidence Zone 3

Fig. 14-1: Allocation of Detail Class and utilisation rate to Confidence Zones

(3) For the various Confidence Zones that signify the confidence in compliance with the requirements that the steel component after hot-dip-zinc coating should be free of cracks if verified with the method given above, the following consequences for inspections have to be considered:

- for Confidence Zone 1 only visual inspections (100 %) are necessary,
 - for Confidence Zone 2 in addition to the visual inspections spot checks using a modified MT-method with adequate sensitivity should be agreed (minimum 1 detail from the relevant detail class per lot) to prove that the full assessment procedure has been safe-sided,
 - for Confidence Zone 3 in addition to the visual inspection a systematic check of steel components should be agreed (minimum 1 detail from each type of detail occurring in Detail Class C per lot) to prove that the full assessment procedure has been safe-sided.
- (4) For complex prefabricated structural components as given in [fig. 14-2](#), the classification may be performed considering the “component method” used in connection design, see EN 1993-1-8. The class with the most onerous detail should be considered as representative for the complete steel component.

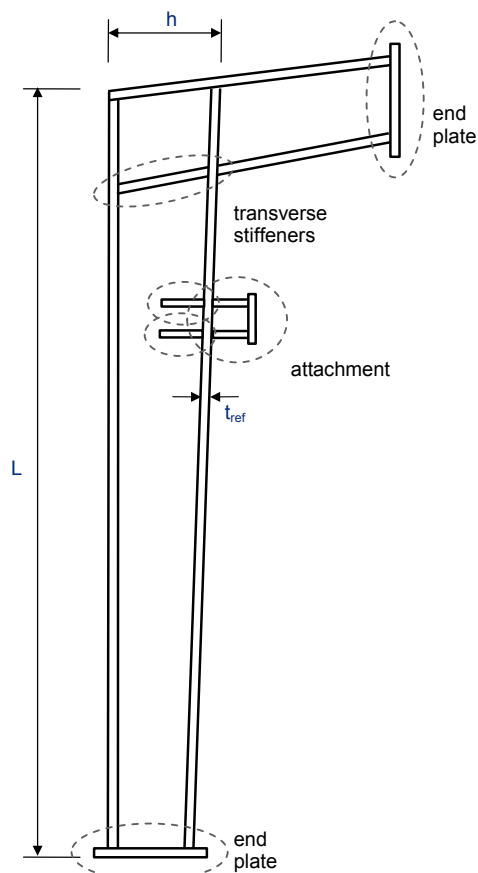


Fig. 14-2: Example for the application of the “component-method” for structural connections to the classification of complex prefabricated steel components

- (5) In order to control the thermal expansion of lattice girders and similar built-up structures it is recommended to avoid excessive instantaneous residual strains due to thermal gradients in the dipping process by segmentation into components with assembly joints.

15 Classification system without numerical assessment

(1) In the following a classification system is derived from the assessment methods in section 13 and section 14 that applies to standard conditions for

- the zinc alloy: zinc alloy class 1, see fig. 7-7,
- dipping speed: 0,8 m/min,
- the preheating temperature: $T_V = 15^\circ\text{C} - 20^\circ\text{C}$,

and to frequently used

- types of construction,
- types of detail,
- plate thicknesses,

assuming ways of fabrication that keep strain-requirements small.

(2) The classification system, that does not need any numerical assessment comprises:

1. classification of construction type,
2. classification of structural detail,
3. classification of predominant product thickness

see fig. 15-1.

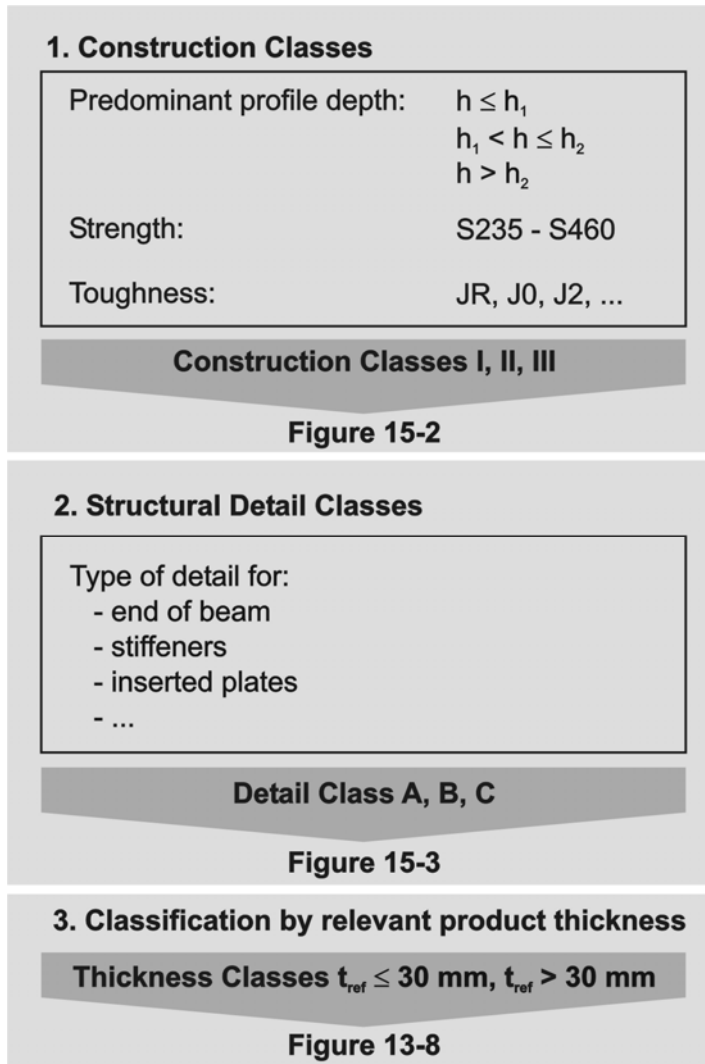


Fig. 15-1: Classification of structural components into Construction Classes, Detail Classes and Thickness Classes

- (3) Fig. 15-2 gives the classification of prefabricated steel components to Construction Classes with a distinction of steel grade, toughness and beam depth.

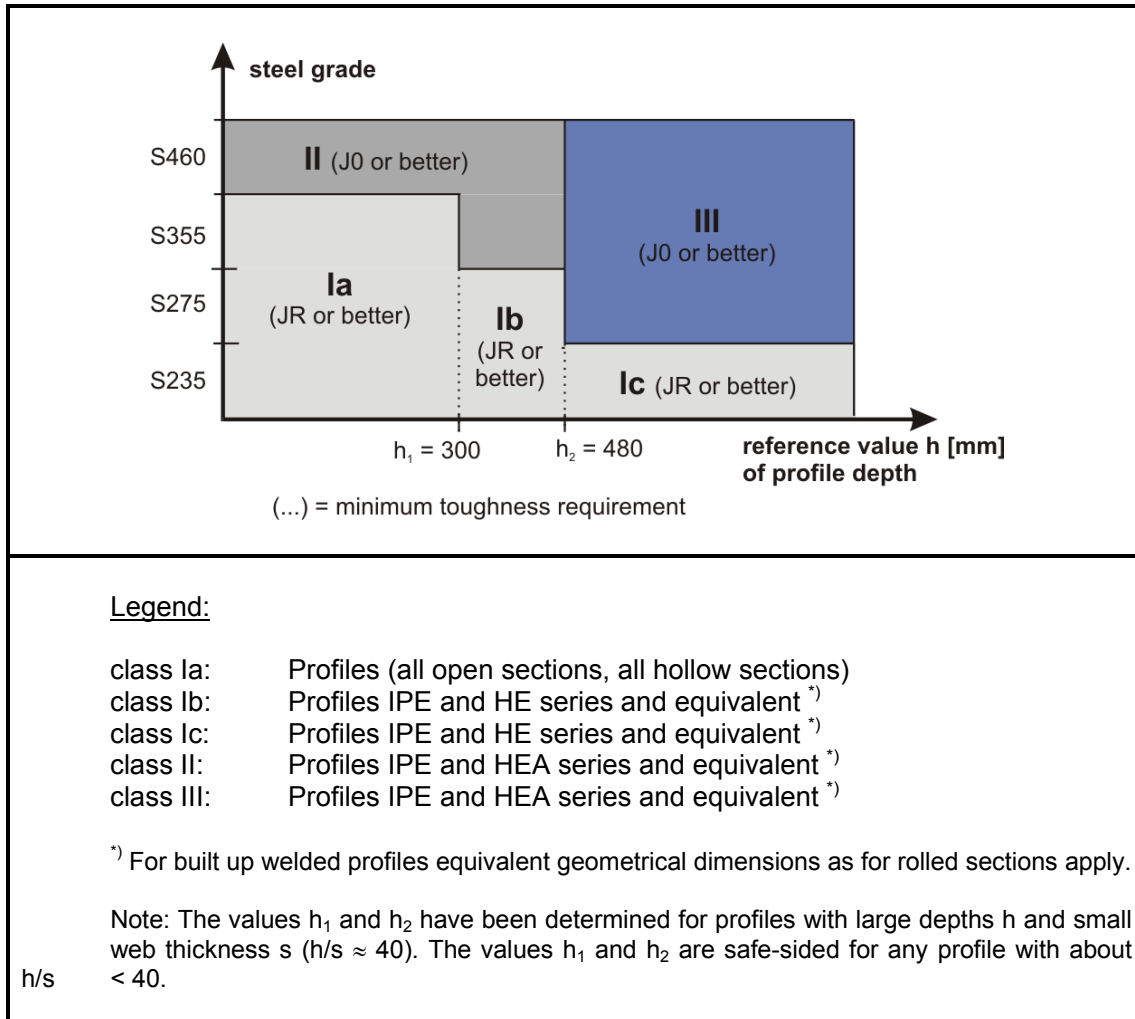


Fig. 15-2: Classification of prefabricated steel components to Construction Classes

- (4) Fig. 15-3 gives a classification of details, where the risk of occurrence of cracks (due to the decrease of safety margin of strain assessment) is the greater the higher the class is (A \rightarrow C). Therefore, the Detail Classes are associated with different Confidence Zones.
- (5) The classification of the predominant product thickness refers to the permissible holding time t_s in fig. 13-8.
- (6) Fig. 15-4 gives the consequences of combination of Construction Class, Detail Class and Thickness Class for the Confidence Zone.

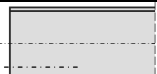
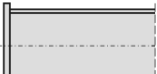


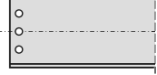
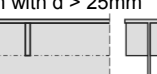

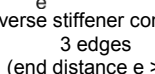

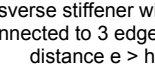
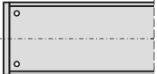
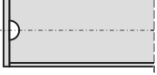
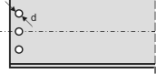
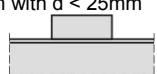
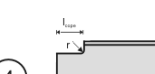
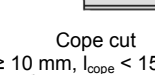


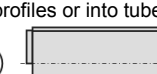

Frequently used typical details where NDT-methods may give indications for cracks		Detail class
<p>①  Free beam end</p> <p>②a </p> <p>②b </p> <p>②c  Full end plates</p> <p>③  Holes in the web at the end of the beam with $d > 25\text{mm}$</p> <p>④  Transverse stiffener ^{*)} connected to 2 edges (end distance $e > h$)</p>	<p>⑤  Transverse stiffener connected to 3 edges (end distance $e > h$)</p> <p>⑥  Transverse stiffener with flange connected to 3 edges (end distance $e > h$)</p> <p>⑦  Transverse stiffener attached to the flange</p> <p>⑧  Shear studs welded to top flange</p> <p>^{*)}drainage holes where necessary in end-plates or stiffeners</p>	A
<p>①a  Drainage holes in the web</p> <p>①b </p> <p>②  Holes in the web at the end of the beam with $d < 25\text{mm}$</p> <p>③  At full welding of fin plates or gusset plates</p>	<p>④  Cope cut $r \geq 10\text{ mm}$, $l_{\text{cope}} < 150\text{ mm}$</p> <p>⑤  Attachments with turn around welds</p> <p>⑥  Attachment with Intermittent welds</p>	B
<p>①  At the weld around plates inserted into the web of profiles or into tubes</p> <p>②  In the web of slender profiles below half cover end plates</p> <p>③  Cope cut $r < 10\text{ mm}$, $l_{\text{cope}} \geq 150\text{ mm}$</p>		C

Fig. 15-3: Classification of details

Confidence of compliance achieved		Confidence zone for dipping process			Check of holding time in zinc melt	
construction class	detail class	A	B	C	$t_{ref} \leq 30 \text{ mm}$	$t_{ref} > 30 \text{ mm}$
		I (a, b, c)	Confidence zone 1			no further check
II	Confidence zone 2	no further check				check required see fig. 13-8
III	Confidence zone 2	Confidence zone 3				no further check

Fig. 15-4: List of combination of classes for achieving confidence in freedom from cracks

16 Worked examples for using the classification method in section 15

16.1 General

- (1) The worked examples presented hereafter demonstrate the use of the classification procedure outlined in section 15 that is based on the choice of
 - zinc alloy class 1,
 - dipping speed 0,8 m/min
 - preheating temperature $T_V = 15^\circ\text{C} - 20^\circ\text{C}$.
- (2) The examples given cover the most frequent cases of structural components to be hot-dip galvanized.

16.2 Usual metal works

- (1) Usual metal works as demonstrated in fig. 16-1 and fig. 16-2 are within the limits of construction class 1a and may be allocated to confidence zone 1 for all detail classes.



© BVM

Figure 16-1: Usual metal works with steel S235JR within the limits of confidence zone 1

(2) The specification for galvanizing is therefore:

- hot-dip galvanizing according to EN ISO 1461 and the standard procedure in section 15
- construction class 1
- only visual inspections.



© BVM

Figure 16-2: Usual metal works with steel S235JR within the limits of confidence zone 1

16.3 Detailed examples

(1) Detailed examples are given in [fig. 16-3](#) to [fig. 16-11](#).

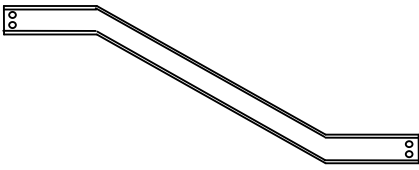
Beams for stairs	material	profile/ beam depth	detail	cold - forming	max. plate thickness t_{ref}
Sketch / description:  <ul style="list-style-type: none"> - welded beam - no welded attachments 	S235JR	U 140	drilled hole $d < 25\text{mm}$	no	$\leq 30\text{mm}$
Assessment for `dipping` detail class: B construction class: Ia	→ confidence zone 1 → no special provisions				
Assessment for `holding`	→ no extra provisions				

Fig. 16-3: Beams for stairs

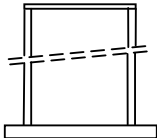
Columns for an industrial building	material	profile/ beam depth	detail	cold- forming	max. plate thickness t_{ref}
Sketch / description:  <ul style="list-style-type: none"> - rolled section with welded footplate - drilled holes in footplate - flange → not relevant 	S235JR	HEA 500	foot plate	no	$\leq 30\text{mm}$
Assessment for `dipping` detail class: A construction class: Ic	→ confidence zone 1 → no extra provisions				
Assessment for `holding`	→ no special provisions				

Fig. 16-4: Columns for an industrial building

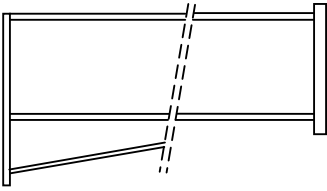
Welded frame beam for an industrial building	material	profile / beam depth	detail	cold-forming	max. plate thickness t_{ref}
Sketch / description:  <ul style="list-style-type: none"> - rolled section with a haunched end and end plates - drilled holes in end plates - flange → not relevant 	S235JR	IPE 500	end plate	no	40mm
Assessment for `dipping` detail class: A construction class: Ic	→ confidence zone 1 → no extra provisions				
Assessment for `holding`	→ limitation of the holding time to 27 min				

Fig. 16-5: Welded frame beam for an industrial building

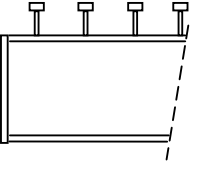
Floor beam for a parking house	material	profile/ beam depth	detail	cold-forming	max. plate thickness t_{ref}
Sketch / description:  <ul style="list-style-type: none"> - rolled section with full endplates - welded shear studs - drilled holes in endplates → not relevant 	S355J2G3	IPE 550	end plate	≤ 0,5%	≤ 30mm
Assessment for `dipping` detail class: A construction class: III	→ confidence zone 1 → no extra provisions				
Assessment for `holding`	→ no special provisions				

Fig. 16-6: Floor beam for a parking house

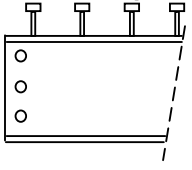
Floor beam for a parking house	material	profile / beam depth	detail	cold-forming	max. plate thickness t_{ref}
Sketch / description:  - rolled section with holes in the web at the end of the beam with $d > 25$ mm - welded shear studs	S460M	IPEa 550	drilled holes, $d > 25$ mm	$\leq 0,5\%$	≤ 30 mm
Assessment for `dipping` detail class: A construction class: III	→ confidence zone 1 → no extra provisions				
Assessment for `holding`	→ no extra provisions				

Fig. 16-7: Floor beam for a parking house

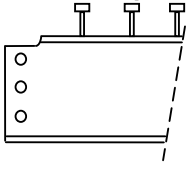
Floor beam for a parking house	material	profile / beam depth	detail	cold-forming	max. plate thickness t_{ref}
Sketch / description:  - rolled section with cope cut - welded shear studs	S460M	IPEa 550	drilled holes, $d > 25$ mm; cope cuts $r < 10$ mm	$\leq 0,5\%$	≤ 30 mm
Assessment for `dipping` detail class: C construction class: III	→ confidence zone 3 → spot wise MT-test in the area of the cope cut				
Assessment for `holding`	→ no extra provisions				

Fig. 16-8: Floor beam for a parking house

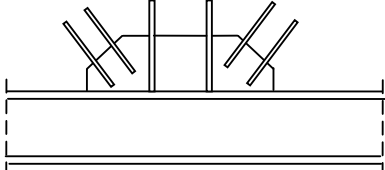
Chord of a truss	material	profile / beam depth	detail	cold-forming	max. plate thickness t_{ref}
Sketch / description:  - rolled section with fin-plate and gusset plates inserted into the fin plate	S355J2	HEB 320	-	no	≤ 30mm
Assessment for `dipping` detail class: C construction class: II	→ confidence zone 2 → spot wise MT-test in the area of welded insertions				
Assessment for `holding`	→ no extra provisions				

Fig. 16-9: Chord of a truss

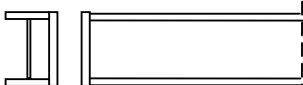
Beam-column connection	material	profile / beam depth	detail	cold-forming	max. plate thickness t_{ref}
Sketch / description:  - rolled beam with end plates - rolled column with connection plate	S235JR	HEA 240	end plate	no	≤ 30mm
Assessment for `dipping` detail class: A construction class: I	→ confidence zone 1 → no extra provisions				
Assessment for `holding`	→ no extra provisions				

Fig. 16-10: Beam-column connection

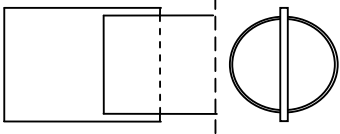
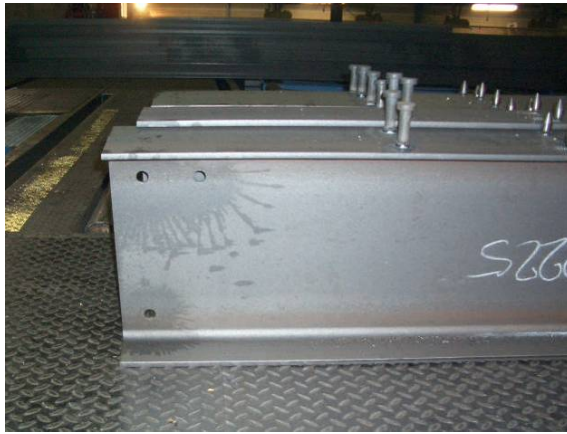
Bracing in a roof	material	profile / beam depth	detail	cold-forming	max. plate thickness t_{ref}
<p>Sketch / description:</p>  <p>- hollow section with inserted gusset plate</p>	S355J2H	273 mm	inserted gusset plate	no	≤ 30mm
<p>Assessment for 'dipping'</p> <p>detail class: C construction class: II</p>	<p>→ confidence zone 2 → spot wise MT-test in the area of insertion of gusset plate</p>				
<p>Assessment for 'holding'</p>	<p>→ no extra provisions</p>				

Fig. 16-11: Bracing in a roof

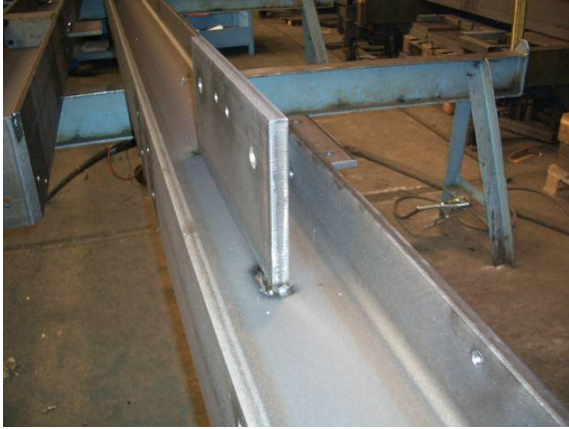
16.4 Examples of choices made in the fabrication



S355J0
Construction class II
Detail class B
→ Confidence zone 1



S235JR
Construction class Ib
Detail class B
→ Confidence zone 1



S235JR
Construction class Ib
Detail class C

→ Confidence zone 1



S355J0
Construction class II
Detail class A
(In case of cold-formed angles with $\varepsilon_{pl} > 2\%$ subject of procedure tests)

→ Confidence zone 1



S355J0
Construction class II
Detail class B

→ Confidence zone 1



S355J0
Construction class II
Detail class C

→ Confidence zone 2



S355J0
Construction class II
Detail class C

→ Confidence zone 2



S235JR
Construction class II
Detail class B

→ Confidence zone 1



S235JR
Construction class I
Detail class B

(In case of cold-formed angles with $\varepsilon_{pl} > 2\%$ subject of procedure tests)

→ Confidence zone 1



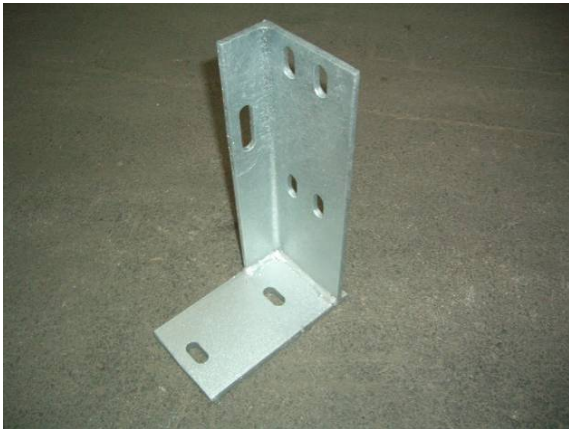
S235JR

Construction class I

Detail class B

(In case of cold-formed angles with $\varepsilon_{pl} > 2\%$ subject of procedure tests)

→ Confidence zone 1



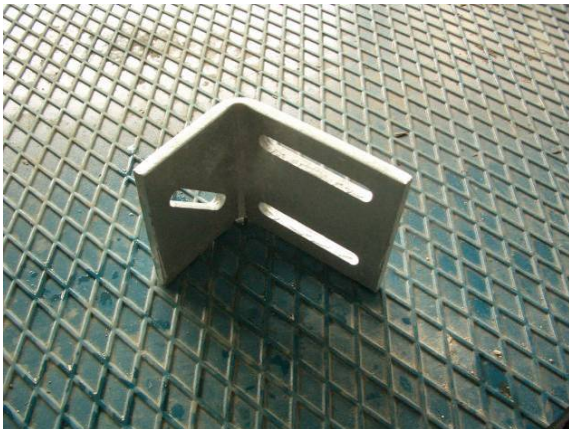
S235JR

Construction class I

Detail class B

(In case of cold-formed angles with $\varepsilon_{pl} > 2\%$ subject of procedure tests)

→ Confidence zone 1



S235JR

Construction class I

Detail class B

(In case of cold-formed angles with $\varepsilon_{pl} > 2\%$ subject of procedure tests)

→ Confidence zone 1



S235JR

Construction class I

Detail class B

(In case of cold-formed angles with $\varepsilon_{pl} > 2\%$ subject of procedure tests)

→ Confidence zone 1



S235JR
Construction class I
Detail class B
(In case of cold-formed angles with $\varepsilon_{pl} > 2\%$ subject of procedure tests)

→ Confidence zone 1



S235JR
Construction class I
Detail class B

→ Confidence zone 1



S355J0
Construction class I
Detail class C

→ Confidence zone 1



S355J0
Construction class I
Detail class A

→ Confidence zone 1



S355J0
Construction class I
Detail class C

→ Confidence zone 1



S355J0
Construction class II
Detail class A

→ Confidence zone 1



S355J0

Construction class I

Cold formed ends with $\varepsilon_{pl} > 2\%$

→ subject of procedure tests

17 Procedure tests

- (1) Where the standard assumptions e.g. related to the aspects in fig. 17-1 which have been made for applying the assessment methods in section 13 to 15 are not met, “procedure tests” with additional non-destructive testing may be applied to achieve hot-dip galvanizing without LMAC.
- (2) The “procedure tests” after acknowledgement identify the particular conditions to be met for the structural detailing, the fabrication of the component and the galvanizing process that have been varied.
- (3) The basis of “procedure tests” is a provisional instruction for galvanizing which comprises all relevant aspects of design, steel products, fabrication and galvanizing procedure and of the NDT to be carried out after galvanizing.
- (4) If the testing is successful the applicant (steel fabricator and zinc coater) may get an acknowledgement according to the legal conditions.

Examples for variations	Extend of NDT
Cold cut edges Cold forming Ratio of plate thickness Structural detailing Latticed structure without joints Longer holding time	Confidence Zone 3 according to <u>fig. 14-1</u> however with testing all details

Figure 17-1: Extend of testing for the procedure tests

18 Supplementary rules for execution of hot-dip-zinc coating

18.1 General

- (1) The assessment methods based on numerical calculations as given in [section 13](#) and [14](#) or based on the classification method as given in [section 15](#) include the concept of confidence zones which require that:
 1. testing of the galvanizing procedure is carried out to secure that the conditions for works as assumed are met and remain stable (independent on time),
 2. testing after the galvanizing process reveals that no cracks have occurred and hence the assessment procedure is safe-sided.
- (2) An important issue of stability of conditions for the galvanizing process is the control of the zinc melt.
- (3) Testing after the galvanizing process is the non destructive testing (NDT) of galvanized components with visual inspections (100 %) and a limited number of MT-tests, where required by the designer (e.g. according to the Confidence Zone resulting from the assessment) or where required after visual tests.
- (4) In the following examples for specifying rules for the control of the zinc melt and for NDT-testing of galvanized components are given, which have been taken from [75].

18.2 Control of chemical composition of the zinc melt

18.2.1 Relevant Standards

- QM-documentation of the zinc coater
- EN ISO 1461
- Requirements for accident prevention

18.2.2 Equipment, tools and sampling

- (1) The outfit for personal protection and the sampling procedure may depend on the regional health and safety requirements.
- (2) Sampling should be carried out from a well mixed zinc bath sufficiently long after measures for maintenance of the zinc bath (e.g. for refurbishment the alloy, etc.).

Note: This requirement would be met if sampling would be made under regular working conditions at least 1 hour after begin of production.

- (3) The sample should be taken always at the same spot of the zinc bath.

Note: E.g. the position should be located at the middle of the long side of the tank, at a distance of 20 cm from the edge and 20 cm below the surface.

Note: A proposal for a device for sampling is given in fig. 18-1. This should be, once the top opened, dipped slowly at an angle to the bath surface until the depth mark is reached.

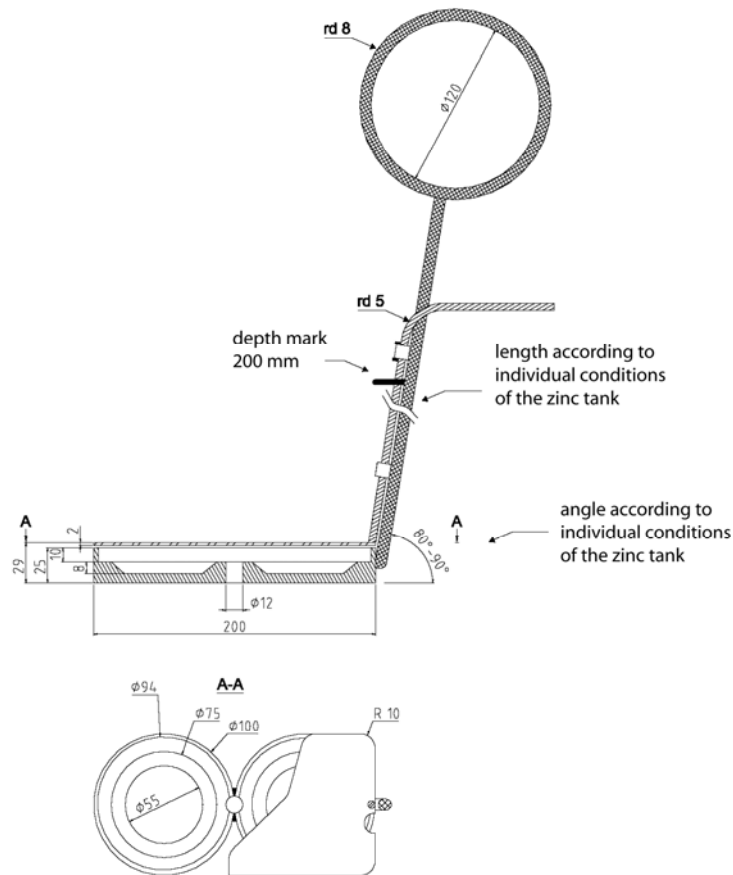


Figure 18-1: Proposal for a device for sampling

- (4) The device for sampling should be moved in the zinc bath sideways (to the right and left) for 2 minutes.
- (5) After that the top of the device should be closed right down by turning.
- (6) The device should be taken out vertically quickly from the zinc bath (Attention to heat protective gloves necessary for regaining one's grip to the hot bar of the sampling device).
- (7) Once outside the zinc tank the bottom part of the sampling device with the samples should be dipped into water, with the samples only partly submerged until solidification and then fully submerged for cooling.
- (8) After cooling the samples should be taken from the device, one for the analysis, the other as reserve for the quality check.
- (9) The samples should be marked with a permanent marker.

- (10) The sampling should be documented in a data sheet for the control documentation.

18.2.3 Method for analysis

- (1) The analysis should only be carried out in laboratories laid down in the QM system.
- (2) The analysis of the zinc sample should give quantitative values for the following elements (8-elements) to characterize sufficiently the composition of the zinc alloy and to check the requirements given in fig. 7-7:
- aluminium (Al)
 - lead (Pb)
 - cadmium (Cd)
 - iron (Fe)
 - copper (Cu)
 - nickel (Ni)
 - bismuth (Bi)
 - tin (Sn)

18.3 Non destructive testing procedures for zinc coated structural components

18.3.1 General

- (1) The non destructive testing (NDT) of zinc coated structural components to detect possible cracks under the zinc coat should be performed with appropriate testing methods, e.g. the magnetic flux tests (MT) taking account of:
- reduced sensitivity from zinc coat thicknesses $t_{Zn} \geq 50 \mu\text{m}$ (see EN 1290, Annex A1)
 - limited accessibility in the area of spandrels from web, flange and endplates.
- (2) The following specification applies to the MT-procedure and contains requirements for the test parameters to achieve an optimum sensitivity for test.

18.3.2 References to standards

EN 473	Qualification and certification of personal for NDT
EN ISO 9934-1	Magnetic flux testing – General basis
EN ISO 9934-2	Magnetic flux testing – Means for testing
EN ISO 9934-3	Magnetic flux testing – Equipment for magnetizing
EN ISO 3059	Magnetic flux testing and penetration testing – Conditions for visual testing

18.3.3 Test personal

- (1) The NDT-checks may only be carried out by qualified personal (at least level II-requirement according to EN 473 for the MT-procedure).

18.3.4 Preparation of surface for testing

- (1) The surfaces should be checked visually (VT) and cleaned where appropriate. Locations where the visual test gives indications should be included in the list of spots prepared by the designer for MT-checks.
- (2) After cleaning, the surfaces for tests should be free of any soiling impeding appropriate testing.

18.3.5 Testing equipment and means for testing

- (1) The testing equipment and the means for testing should comply with the relevant standards.

18.3.6 Check of sufficient magnetizing of the testing system

- (1) Sufficient magnetizing of the steel surface should be achieved by an appropriate level of the strength of the magnetic field.
- (2) The magnetizing should be checked by measuring the tangential strength of the magnetic field.

The strength measured as closely as possible at the surface on the basis of the Hall-effect should attain a value of 4 kA/m (40 A/cm).

- (3) Electric power generators used should give sufficient power supply.

18.3.7 Check of sufficient magnetizing for a project

- (1) Before starting the test works (at least once a day) the magnetizing should be checked with a reference component.

18.3.8 Means for testing

- (1) The means for testing should comply with the requirements of EN ISO 9934-2 and the particular conditions from reduced sensitivity by the zinc coat.

Note: The following means for testing have proved to be suitable:

- MR 76 MR-Chemie
- NRS 107 Helling
- Ferroflux-Pulver-Suspension 690.2

18.3.9 Visual evaluation

- (1) The following conditions apply for the visual evaluation using black means of testing:
 - the surface should be controlled with an illumination strength of at least 500 Lux.

18.3.10 Area to be tested

- (1) The areas to be tested should be determined by the designer, see [fig. 18-2](#). These areas should be supplemented by spots where visual testing has identified indications.
- (2) Magnetizing should be achieved by hand-magnets. Sufficient time for post-magnetizing should be taken into account.

Note: A sufficient time for magnetizing of 6 s and a subsequent post magnetizing time of 6 s would provide sufficient time for the formation of indications.

- (3) The overlapping of areas to be tested should be sufficient.

18.3.11 Limits for confidence

- (1) Linear indications caused by material discontinuities (e.g. cracks, fusion lacks, flow over of weld material) are not permitted.
- (2) Where the existence of cracks is suspected, the test should be performed without the zinc coat after grinding.
- (3) Unless otherwise specified by the designer indications with lengths ≤ 3 mm may be disregarded.

Note: In areas with high local plastic strains which may occur in the parent material by weld-shrinkage adjacent to large welds, indications may be found inspite of fulfilling all conditions to avoid LMAC. In case of such indications, it has to be decided whether these indications mean through cracks or only surface cracks and whether further measures, e.g. grinding, is necessary.

18.3.12 Demagnetizing

- (1) A demagnetizing of welded structural components normally is not necessary.

18.3.13 Treatment of structural components with faults

- (1) Any decision for the treatment of structural components with faults should be made together with the designer.

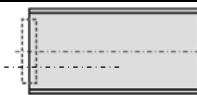
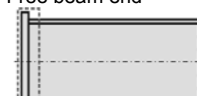
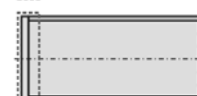
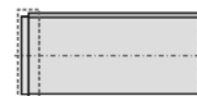





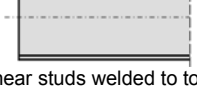


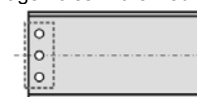
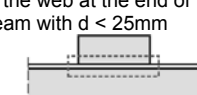
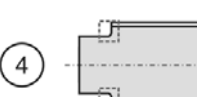
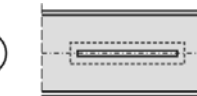
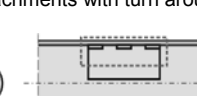
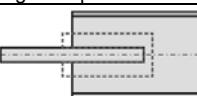
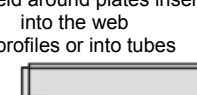

Frequently used typical details where NDT-methods may give indications for cracks		Detail class
<p>① Free beam end</p>  <p>②a</p>  <p>②b</p>  <p>②c Full end plates</p>  <p>③ Holes in the web at the end of the beam with $d > 25\text{mm}$</p>  <p>④ Transverse stiffener ¹⁾ connected to 2 edges (end distance $e > h$)</p> 	<p>⑤ Transverse stiffener connected to 3 edges (end distance $e > h$)</p>  <p>⑥ Transverse stiffener with flange connected to 3 edges (end distance $e > h$)</p>  <p>⑦ Transverse stiffener attached to the flange</p>  <p>⑧ Shear studs welded to top flange</p>  <p>¹⁾drainage holes where necessary in end-plates or stiffeners</p>	A
<p>①a</p>  <p>①b Drainage holes in the web</p>  <p>② Holes in the web at the end of the beam with $d < 25\text{mm}$</p>  <p>③ At full welding of fin plates or gusset plates</p> 	<p>④ Cope cut $r \geq 10\text{ mm}$, $l_{\text{cope}} < 150\text{ mm}$</p>  <p>⑤ Attachments with turn around welds</p>  <p>⑥ Attachment with intermitted welds</p> 	B
<p>① At the weld around plates inserted into the web of profiles or into tubes</p>  <p>② In the web of slender profiles below half cover end plates</p> 	<p>③ Cope cut $r < 10\text{ mm}$, $l_{\text{cope}} \geq 150\text{ mm}$</p> 	C

Figure 18-2: Areas to be tested

18.3.14 Documentation of the tests

- (1) The documentation of the tests should comply with the requirements in EN ISO 9934-1.
- (2) The location and the sizes of faults should be clearly documented.

19 Conclusion

- (1) This JRC-Scientific and Technical Report gives a survey on the state-of-the-art in explaining the causes of liquid metal assisted cracking (LMAC) of prefabricated structural steel components in the zinc melt during hot-dip galvanizing that may impair their structural safety. It also offers ways to avoid it.
- (2) Various parameters related to:
 - the design of prefabricated components,
 - the fabrication of prefabricated component,
 - the zinc alloy and the galvanizing process.

control the likelihood for occurrence of this phenomenon, so that information across design, fabrication and galvanizing need to be taken into account to produce hot-dip-galvanized structural components that are free from cracks.

- (2) This report also demonstrates mechanical models suitable to consider cracking in the zinc melt as a limit state related to plastic strain requirements on one side and ultimate plastic strain resistances on the other side.
- (3) To determine such plastic strain resistances a new testing procedure with small scale LNT-test specimen has been developed, that reveals the interaction between the steel material, zinc alloy and galvanizing process and time. To determine plastic strain requirements numerical simulations of the “stationary” strain field from the fabrication of components and of the “non-stationary” strain fields from the dipping and holding processes are necessary.
- (4) For practical use simplified methods have been derived from the results of such limit state studies, either with simplified mechanical models for numerical assessment or with classification methods, that do not need any calculation. These models are based on standardized conditions for:
 - choice of profiles and steel,
 - structural detailing considering notch effects,
 - galvanizing process,
 - inspection and testing.
- (5) Due to various uncertainties related to compliance with these conditions and to the simplified assessment model used, confidence zones are introduced for which rules for inspection and non-destructive testing are defined, so that the combination of assessment and testing produces the reliability required for avoiding liquid metal assisted cracking.
- (6) Worked examples complete the survey; they give proof that the methods developed are workable and applicable to practical use.

20 Literature

- [1] Mitteilungen des Bayerischen Staatsministeriums des Inneren; Rissbildung an feuerverzinkten Stahlkonstruktionen, 24.05.2006 sowie ähnliche Mitteilungen der Obersten Baubehörden anderer Bundesländer
- [2] Weber, L., Hoffmann, J.: Communiqué der Fa. Arcelor-Mittal zur Verzinkungsrisss-Problematik, 2007
- [3] Katzung W., Schulz W.-D.: Beitrag zum Feuerverzinken von Stahlkonstruktionen - Ursachen und Lösungsvorschläge zum Problem der Rissbildung. Stahlbau 74 (2005), S. 258-273
- [4] Breitschaft, G., Ulbrich D.: Rissbildung in feuerverzinkten Stahlkonstruktionen, DIBt Mitteilungen, 37 (2006) 6, S. 219-221
- [5] DIN EN 1290: Zerstörungsfreie Prüfung von Schweißverbindungen – Magnetpulver-Prüfung von Schweißverbindungen, September 2002
- [6] Feldmann M., Pinger T., Tschickardt D.: Ursachen und Einflüsse auf die Rissbildung beim Feuerverzinken von großen Stahlkonstruktionen, GAV-Forschungskolloquium Hannover 2007
- [7] Nies, H., Schambiel, G., Stiefel, B.: Die Problematik der Rissbildung beim Feuerverzinken, Der Praktiker – DVS Verlag, Seite 178 – 185, 6/2007
- [8] Feldmann M., Pinger T., Tschickardt D.: Cracking in large steel structures during hot dip galvanizing. Intergalva 2006, Neapel 2006
- [9] Kinstler, T J.: Current Knowledge of the Cracking during Galvanizing, Galva Science LLC, Canada, 2005
- [10] Feldmann M.: Feuerverzinken von großen Stahlkonstruktionen; Risssschäden – Ursache, Hintergründe und Vermeidung, Gemeinschaftsausschuss Feuerverzinken e.V., Forschungskolloquium Wiesbaden, Nov. 2003
- [11] Feldmann M.: A new Aspect of Crack Assessment of Galvanized Steel Structures, 4th Eurosteel Conference, Maastricht (NL), May 2005
- [12] Sedlacek G., Dahl W., Hoffmeister B., Kühn B., Feldmann M., Pinger T., Langenberg P., Blum M., Grotmann D., Eichenmüller H.: Zur sicheren Anwendung feuerverzinkter Träger. Stahlbau 73 (2004), S. 427-437
- [13] Herold, H.; Woywode, N.; Pieschel, J.: Fertigungsbedingte Risse durch ungünstige schweißtechnische Gestaltung und Ausführung, Z. Metallk., S.232-236, 2001
- [14] Pargeter, R.: Liquid metal penetration during hot dip galvanizing, Internetveröffentlichung, The Welding Institute, Great Abington, Cambridge, 2003
- [15] Herbsleb, G.; Pöpperling, R.: Dehnungsinduzierte Spannungsrisskorrosion an Stählen, Werkstoffe und Korrosion 29 (1978) S. 732-739
- [16] Engell, H.-J.; Speidel, M. O.: Ursachen und Mechanismen der Spannungsrisskorrosion, Werkstoffe und Korrosion 20 (1969) S. 281-300
- [17] Friehe, W.: Dehnungsinduzierte Spannungsrisskorrosion in Flüssigmetallen, Werkstoffe und Korrosion 29 (1978) S. 747-753
- [18] Old, C. F.; Trevena, P.: Embrittlement of zinc by liquid metals, Metal Science, p. 487-495, 1979
- [19] Old, C. F.: Liquid metal embrittlement of nuclear materials, Journal of nuclear materials 92, p. 2-25, 1980
- [20] Old, C. F.: Micromechanisms of crack growth in liquid metal environments, Metal science, p. 433-440, 1980
- [21] Rostoker, W.; McCaughey, J. M.; Markus, H.: Embrittlement by Liquid Metals, Reinhold Publishers, New York, 1960

- [22] Westwood, A. R. C.; Kamdar, M. H.: In Environment Sensitive Mechanical Behaviour, A. R. C. Westwood and N. S. Stoloff, Ed., TMS-AIME Conference 35, Gordon and Breach, 1966 p. 581
- [23] Pargeter, F. W. J.; Ives, M. B.: Grain Size Dependence of Fracture in Copper-Aluminium Alloys Embrittled by Mercury, Canadian Journal of Physics 45, p. 1234, 1967
- [24] Hancock, P. C.; Ives, M. B.: The role of plastic deformation in liquid metal embrittlement, Canadian metallurgical quarterly, Volume 10, 1971
- [25] Rädeker, W.: Die Erzeugung von Spannungsrissen in Stahl durch flüssiges Zink, Stahl u. Eisen 73 (1953), S. 654-658
- [26] Nieth, F.: Festigkeitsfragen im Zusammenhang mit der Feuerverzinkung, Dissertation D17, Darmstadt, 1965
- [27] Funke, P.; Klemens, D.: Untersuchung über den Einfluss des Zinks und seiner Legierungselemente auf die Rissbildung von Stählen, TU Clausthal, Projekt im Rahmen des Forschungs- und Entwicklungsprogramm „Korrosion und Korrosionsschutz, 1980
- [28] Klemens, D.: Inbetriebnahme von Verzinkungskesseln, Spannungen im Kesselmaterial und Rissgefährdung durch unterschiedliche Zinkschmelzen. Gemeinschaftsausschuss Verzinken e.V. Düsseldorf, Vortrags- und Diskussionsveranstaltung GAV 1983
- [29] Schwenk, W. „Einflussgrößen bei der Korrosion von Stählen unter Rissbildung mit besonderer Berücksichtigung der mechanischen Belastungsparameter“ in Festigkeitsverhalten höherfester schweißbarer Baustähle / Korrosion“, VEB Deutscher Verlag für Grundstoffindustrie, Leipzig, 1983
- [30] Herbsleb, G.; Pfeiffer, B.; Pöpperling, R.; Schwenk, W.: Die Wirkung mechanischer Einflussgrößen bei der Risskorrosion von Kohlenstoff-Mangan-Stählen, Z. Werkstoff-tech, 1978
- [31] Schubert, P.; Schulz, W.-D.; Katzung, W.; Rittig, R.: Struktur und Eigenschaften von Feuerzinküberzügen, Metall 53, S. 260-268, 1999
- [32] Merkblatt 329 - Korrosionsschutz durch Feuerverzinken (Stückverzinken), Stahl-Informationen-Zentrum und Gemeinschaftsausschuss Verzinken e.V., Düsseldorf
- [33] Sandelin, R. W.: Galvanizing characteristics of different types of steel, Wire and Wire Products No. 12, 1940
- [34] Klemens, D., Kaszás, S.: Untersuchung der Spannungsrisskorrosion von Baustählen in flüssigem Zink. Werkstoffe und Korrosion 43(1992), 561-564.
- [35] Nürnberger, U.; Menzel, K.: „Rissbildung beim Feuerverzinken von Feinkornbaustählen“, Abschlussbericht in der Forschungs- und Materialprüfungsanstalt Baden-Württemberg, 1998
- [36] Kikuchi, M.: Liquid metal embrittlement of steels by molten zinc, Proceedings of the 23rd Japan Congress on Material Research, 1980
- [37] Kikuchi, M.; Lezawa, T.: Liquid Metal Embrittlement of Steels in Molten Zinc, Journal of the Society of Naval Architects, Japan, Vol. 149, No. 6, 1981, pp. 298-305
- [38] Kikuchi, M.: Study on fracture mechanisms of liquid metal embrittlement cracking of steels in molten zinc, Proceedings of the 24th Japan Congress on Material Research, 1981
- [39] Kikuchi, M.: Liquid Metal Embrittlement Cracking of Notched Rectangular Steel Plate in Molten Zinc, Journal of the Society of Materials Science, Japan, Vol. 30, No. 329, 1981, pp. 194-199
- [40] Kikuchi, M.: Liquid Metal Embrittlement of Steels during Hot Dip Galvanizing, Tetsu to Hagane, (Iron and Steel), Vol. 68, Number 14, 1982, p. 1870-1879

- [41] Abe, H.; Lezawa, T.; Kanaya, K.; Yamashita, T.; Aihara, S.; Kanazawa, S.: Study of HAZ cracking of hot-dip galvanizing steel bridges, International Institute of Welding, IIW Doc. IX-1795-94
- [42] Kikuchi, M.; Lezawa, T.: Effect of Stress-Concentration Factor on Liquid Metal Embrittlement Cracking of Steel in Molten Zinc, Journal of the Society of Materials Science, Japan, Vol. 31, No. 352, 1982, p. 271-276
- [43] Kikuchi, M.: Prevention of distortion and of crack initiation, Proceedings 13th International Galvanizing Conference, London, 1982, European General Galvanizers Association
- [44] Bargel, H.-J., Schulze, G., Cev Gülec, S., Aran, A.: Malzene Bilgisi, Cilt II, J.T.Ü. Makina Fakültesi, Istanbul, 1995
- [45] DIN EN 10025: Warmgewalzte Erzeugnisse aus Baustählen, 2006
- [46] DIN EN 1461: Durch Feuerverzinken auf Stahl aufgebrachte Zinküberzüge (Stückverzinken) – Anforderungen und Prüfungen, März 1999
- [47] DAST- Richtlinie 009:2005-01: Stahlsortenauswahl für geschweißte Stahlbauten, Deutscher Stahlbauverband, Stahlbau Verlags- und Service GmbH, Düsseldorf, 2005
- [48] DIN EN 1993-1-10:2005-07: Eurocode 3: Bemessung und Konstruktion von Stahlbauten- Teil 1-10: Stahlsortenauswahl in Hinblick auf Bruchzähigkeit und Eigenschaften in Dickenrichtung, Bemessungsregeln für den Stahlbau, Beuth-Verlag, Berlin, 2005
- [49] Peil, U.; Wichers, M.: Schweißen unter Betriebsbeanspruchungen – Werkstoffkennwerte für einen S355J2G3 unter Temperaturen bis 1200°C, Stahlbau 73 (2004), H. 6, S. 400-416
- [50] Feldmann M., Bleck W., Langenberg P., Pinger T., Tschickardt D., Völling A., Ermittlung der Rissanfälligkeit beim Stückverzinken, MP Materials Testing 49 (2007), S. 223-231
- [51] Petersen, C.: Stahlbau – Grundlagen der Berechnung und baulichen Ausbildung von Stahlbauten, Vieweg & Sohn Verlagsgesellschaft mbH, 1993
- [52] Roik, K.: Vorlesungen über Stahlbau, Verlag Ernst & Sohn, 1983
- [53] Malisius, R.: Schrumpfungen, Spannungen und Risse beim Schweißen, Deutscher Verlag für Schweißtechnik (DVS), Düsseldorf, 1957
- [54] Nitschke- Pagel, T.; Dilger, K.: Eigenspannungen in Schweißverbindungen – Teil 1: Ursachen der Eigenspannungsentstehung beim Schweißen, Verlag für Schweißen und verwandte Verfahren, Düsseldorf, Schweißen und Schneiden 58 (2006), H.9, S. 466-479
- [55] Radaj, D.: Wärmewirkungen des Schweißens, Temperaturfeld, Eigenspannungen, Verzug. Springer-Verlag, Berlin, 1988
- [56] Nitschke-Pagel, T., Wohlfahrt, H: Residual stresses in welded joints - sources and consequences. Proc. 6. European Conference on Residual Stresses S.215/24. Trans Tech Publications, Suisse 2002
- [57] Pinger, T.: Zur Vermeidung der Rissbildung an Stahlkonstruktionen beim Feuerverzinken bei besonderer Berücksichtigung der flüssigmetallinduzierten Spannungsrisskorrosion, Diss. RWTH Aachen, 2009
- [58] Neuber, Heinz: Kerbspannungslehre - Theorie der Spannungskonzentration; genaue Berechnung der Festigkeit. Berlin, u.a.: Springer, 1985
- [59] Galvanizing Structural Steelwork – An approach to the management of liquid metal assisted cracking, BCSA and GA publication No. 40/05
- [60] Empfehlungen zur Prüfung feuerverzinkter Stahlkonstruktionen mittels modifiziertem MT-Verfahren, Lehrstuhl für Stahlbau, RWTH Aachen, 2006

- [61] Prüfanweisung für die zerstörungsfreie Prüfung von geschweißten feuerverzinkten Stützenjochen Ausführung 98, Nr. PAST0100, Doppelmayr Seilbahnen GmbH, Wolfurt
- [62] DIN 18800 - 1: Stahlbauten - Bemessung und Konstruktion, November 1990
- [63] DIN 18800 – 7: Stahlbauten – Ausführung und Herstellerqualifikation, September 2002
- [64] DIN EN ISO 5817: Schweißen – Schmelzschweißverbindungen an Stahl, Nickel, Titan und deren Legierungen (ohne Strahlschweißen) – Bewertungsgruppen von Unregelmäßigkeiten (ISO 5817:2003 + Cor. 1:2006); Deutsche Fassung EN ISO 5817:2003 + AC:2006
- [65] Vermeidung von Rissen beim Feuerverzinken von großen Stahlkonstruktionen mit hochfesten Stählen, GAV-AiF- Forschungsvorhaben 14545 N/1, Lehrstuhl für Stahlbau und Leichtmetallbau und Institut für Eisenhüttenkunde, RWTH Aachen, Abschlussbericht 2007
- [66] RFCS- Forschungsprojekt TGS5 – RFS CR 03021 „Failure Mechanisms During Galvanizing – FAMEGA“, Aachen, Rotherham, Esch-sur-Alzette, Kaiserslautern, Santander, Abschlussbericht 2007
- [67] Rädeler, W.; Haarmann, R.: Angriffsarten des Zinks auf Stahl bei der Feuerverzinkung, Stahl und Eisen 59 (1939), S. 1217-1227
- [68] Breitschaft, G.: Schäden an feuerverzinkten Stahlkonstruktionen, Schreiben vom 09.05.2006
- [69] Rädeler, W.: Der interkristalline Angriff von Metallschmelzen auf Stahl, Werkstoffe und Korrosion 24 (1973), S. 851-859
- [70] „Konstruktionsgerechtes Verzinken, verzinkungsgerechtes Konstruieren“, DAST-Richtlinie 022, in Vorbereitung
- [71] Markus Feldmann, Thomas Pinger, Dirk Tschickardt, Peter Langenberg, Alexander von Richthofen, Peter Karduck: Rissbildung durch Flüssigmetallversprödung beim Feuerverzinken von Stahlkonstruktionen. In: Stahlbau-Kalender, hrsgn. von U. Kuhlmann. Berlin: Ernst & Sohn 2008
- [72] Markus Feldmann, Thomas Pinger, Dirk Tschickardt, Wolfgang Bleck, Alexander Völling, Peter Langenberg: Analyse der Einflüsse auf die Rissbildung infolge Flüssigmetallversprödung beim Feuerverzinken, Stahlbau 77 (2008), S. 46-61
- [73] Markus Feldmann, Thomas Pinger, Gerhard Sedlacek, Dirk Tschickardt: Die neue DAST-Richtlinie zur Vermeidung von Rissbildung beim Feuerverzinken, Stahlbau 77 (2008), S. 734-742
- [74] Kinstler, T.J.: Current knowledge of the cracking of steels during galvanizing. GalvaScience for AISC
http://www.aisc.org/Content/ContentGroups/Engineering_and_Research/Research1/Final5906.pdf
- [75] DAST-Richtlinie 022 – Feuerverzinken von tragenden Stahlbauteilen, Deutscher Ausschuß für Stahlbau, October 2009

European Commission

EUR 24286 EN – Joint Research Centre – Institute for the Protection and Security of the Citizen

Title: Hot-dip-zinc-coating of prefabricated structural steel components
Author(s): M. Feldmann, T. Pinger, D. Schäfer, R. Pope, W. Smith, G. Sedlacek
Luxembourg: Office for Official Publications of the European Communities
2010 – 102 pp. – 21 x 29.7 cm
EUR – Scientific and Technical Research series – ISSN 1018-5593
ISBN 978-92-79-15237-5
DOI 10.2788/73644

Abstract

This JRC-Scientific and Technical Report gives information from pre-normative research for methods to prevent liquid metal assisted cracking of prefabricated structural components during zinc-coating in the liquid zinc melt, that may impair the structural safety of structures in which the components are built in. This information provides a platform upon which further European design and product specifications can be developed. It may in particular affect the further developments of EN 1993, EN 1090, EN ISO 1461 and EN ISO 14713.

This report gives the state-of-the-art in understanding the mechanism of liquid metal assisted cracking in the zinc bath and methods and models that may be used to avoid it. It could be a basis to propose rules for the design of steel components intended to be hot-dip-zinc-coated in such a way that the design is consistent with execution rules for hot-dip-zinc-coating. The workability of the rules proposed for all metal works and steel works that are fabricated under EN 1090 and galvanized according to the rules in this report is demonstrated by worked examples.

How to obtain EU publications

Our priced publications are available from EU Bookshop (<http://bookshop.europa.eu>), where you can place an order with the sales agent of your choice.

The Publications Office has a worldwide network of sales agents. You can obtain their contact details by sending a fax to (352) 29 29-42758.

The mission of the JRC is to provide customer-driven scientific and technical support for the conception, development, implementation and monitoring of EU policies. As a service of the European Commission, the JRC functions as a reference centre of science and technology for the Union. Close to the policy-making process, it serves the common interest of the Member States, while being independent of special interests, whether private or national.

LB-NA-24286-EN-C

